The metamorphic sole of New Caledonia ophiolite: $^{40}Ar/^{39}Ar$, U-Pb, and geochemical evidence for subduction inception at a spreading ridge

Dominique Cluzel,[1] Fred Jourdan,[2] Sébastien Meffre,[3] Pierre Maurizot,[4] and Stéphane Lesimple[5]

Received 21 December 2011; revised 24 April 2012; accepted 26 April 2012; published 13 June 2012.

[1] Amphibolite lenses that locally crop out below the serpentinite sole at the base of the ophiolite of New Caledonia (termed Peridotite Nappe) recrystallized in the high-temperature amphibolite facies and thus sharply contrast with blueschists and eclogites of the Eocene metamorphic complex. Amphibolites mostly display the geochemical features of MORB with a slight Nb depletion and thus are similar to the youngest (Late Paleocene–Eocene) BABB components of the allochthonous Poya Terrane. Thermochronological data from hornblende ($^{40}Ar/^{39}Ar$), zircon, and sphene (U-Pb) suggest that these mafic rocks recrystallized at ~56 Ma. Using various geothermobarometers provides a rough estimate of peak recrystallization conditions of ~0.5 GPa at ~800–950°C. The thermal gradient inferred from the metamorphic assemblage (~60°C km^{-1}), geometrical relationships, and geochemical similarity suggest that these mafic rocks belong to the oceanic crust of the lower plate of the subduction/obduction system and recrystallized when they subducted below young and hot oceanic lithosphere. They were detached from the down-going plate and finally thrust onto unmetamorphosed Poya Terrane basalts. This and the occurrence of slab melts at ~53 Ma suggest that subduction inception occurred at or near to the spreading ridge of the South Loyalty Basin at ~56 Ma.

Citation: Cluzel, D., F. Jourdan, S. Meffre, P. Maurizot, and S. Lesimple (2012), The metamorphic sole of New Caledonia ophiolite: $^{40}Ar/^{39}Ar$, U-Pb, and geochemical evidence for subduction inception at a spreading ridge, *Tectonics*, *31*, TC3016, doi:10.1029/2011TC003085.

1. Introduction

[2] The concept of ophiolite has greatly evolved since its first use by A. Brongniart in the early 19th century, the abandonment in the 1970s of the co-magmatic model, and acceptation of obduction as the principal tectonic mechanism of ophiolite genesis [*Coleman*, 1971]. At present, there is a consensus to consider that ophiolites may represent either supra-subduction (upper plate) rocks emplaced when a buoyant unit blocked the subduction zone (the Tethyan-type ophiolites), or alternatively, by lower plate rocks interleaved or thrust above subduction complexes (the Cordilleran-type ophiolites) (for a review, see *Dilek* [2003] and *Wakabayashi and Dilek* [2003]).

[3] Metamorphic rock units that sporadically crop out at the base of Tethyan-type ophiolites (and referred to as metamorphic soles) record a variety of thermal regimes, which are inconsistent with the high-pressure low-temperature (HP-LT) gradient that usually prevails in subduction zones. However, with only a few exceptions, tectonic models for that type of ophiolite emplacement advocate that subduction precedes obduction (the blocked subduction model) with HP-LT metamorphic complexes (blueschist and eclogite facies rocks) forming at great depth beneath the upper plate (for a review, see *Lippard* [1983], *Platt* [1993], *Chemenda et al.* [1996], *Wakabayashi and Dilek* [2000, 2003], *Dilek* [2003], and *Yamato et al.* [2007, and references therein]). Metamorphic soles of ophiolitic complexes are dominantly composed of amphibolite with subordinate metasediments, which are generally interpreted as metamorphosed lower plate rocks. These metamorphic rocks are thought to form when oceanic crust subducts below young and hot oceanic lithosphere and signal subduction inception at or near to a spreading ridge [*Nicolas*, 1989; *Boudier et al.*, 1988]. However, such an

[1]Pôle Pluridisciplinaire de la Matière et de l'Environnement, Université de la Nouvelle-Calédonie, Nouméa, New Caledonia.
[2]Western Australian Argon Isotope Facility, Department of Applied Geology and John de Laeter Centre for Isotope Research, Curtin University of Technology, Perth, Western Australia, Australia.
[3]Australian Research Council Centre of Excellence in Ore Deposits, University of Tasmania, Hobart, Tasmania, Australia.
[4]Bureau de Recherches Géologiques et Minières, Nouméa, New Caledonia.
[5]Direction de l'Industrie, des Mines et de l'Energie, Service Géologique de la Nouvelle-Calédonie, Nouméa, New Caledonia.

Corresponding author: D. Cluzel, Pôle Pluridisciplinaire de la Matière et de l'Environnement, Université de la Nouvelle-Calédonie, EA 3325, BP R4, 98851 Nouméa CEDEX, New Caledonia. (dominique.cluzel@univ-nc.nc)

©2012. American Geophysical Union. All Rights Reserved.

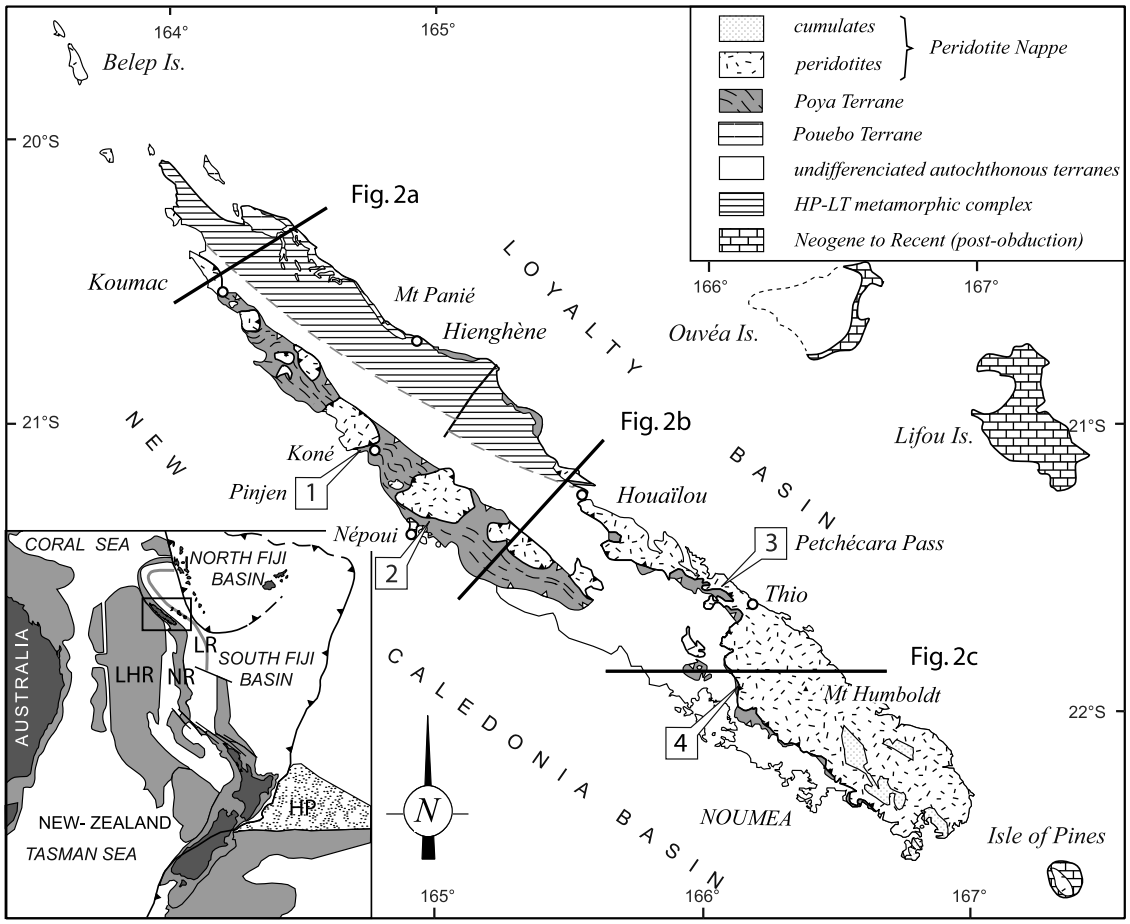

Figure 1. Geological sketch map of New Caledonia to show the location of amphibolite lenses, the mafic (Poya Terrane) and ultramafic (Peridotite Nappe) allochthons, and the HP-LT metamorphic complex units (low grade to the SW and high grade to the NE). Inset shows the structure of the Southwest Pacific Region. Dark gray, land; light gray, continental plateau; white, oceanic basins (LHR: Lord Howe Rise; NR: Norfolk Ridge; LR: Loyalty Ridge; HP: Hikurangi Plateau).

interpretation does not fit the P-T-t features of all metamorphic soles so far, and detailed genetic models are still a matter of debate (for a review, see *Searle and Cox* [2002], *Robertson* [2004], and *Boudier and Nicolas* [2007, and references therein]). As ophiolites and associated rocks are very diverse, an accurate knowledge of age, protoliths, and thermal regimes of associated metamorphic rocks is critical for constraining genetic models for obduction and subduction initiation [i.e., *Smart and Wakabayashi*, 2009; *Wakabayashi et al.*, 2010].

[4] A very important geological feature of New Caledonia is the large ultramafic allochthon [*Avias*, 1967] currently termed Peridotite Nappe, or New Caledonia Ophiolite (Figure 1). These upper mantle rocks are thought to represent the on land allochthonous extension of the Loyalty Basin [*Collot et al.*, 1987]. The upper crustal rocks of this obducted oceanic lithosphere do not crop out and were likely eroded during pre- and post-obduction uplift as well. Because of the extremely low concentrations of incompatible elements in these highly depleted rocks, very few radio-chronologic and time constraints exist concerning the formation of the ultramafic allochthon [*Prinzhoffer*, 1981, 1987; *Cluzel et al.*, 2006] and its obduction [*Cluzel et al.*, 1998; *Paquette and Cluzel*, 2007]. Moreover, there is still no general agreement about the tectonic process that led to obduction. Some authors consider that a west dipping subduction preceded obduction [e.g., *Sutherland et al.*, 2010]; however, a model of blocked northeast- or north-northeast-dipping subduction is generally preferred [*Parrot and Dugas*, 1980; *Aitchison et al.*, 1995a; *Cluzel et al.*, 2001, 2006; *Crawford et al.*, 2003; *Schellart et al.*, 2006]. Subduction initiation is also poorly constrained with previous studies, suggesting subduction inception along a transform fault [*Paris*, 1981], along the eastern margin of the Norfolk ridge [*Sutherland et al.*, 2010], or alternatively, at or near the spreading ridge of the South Loyalty basin, to the east of Norfolk ridge [*Ulrich et al.*, 2010]. Differentiating between these various hypotheses requires more robust time-constraints.

[5] Genetic and emplacement models of the Peridotite Nappe have overlooked the amphibolite lenses that crop out locally at its base [see *Paris*, 1981; *Prinzhoffer*, 1981, 1987; *Collot et al.*, 1987]. This article presents the first geochemical and thermochronological data on these metamorphic rocks and provides new constraints on subduction/obduction models for the Peridotite Nappe.

[6] Stages names and limits used in the text refer to the Geological Society of America geological timescale of J. D. Walker and J. W. Geissman (2009 Geologic Time Scale, 2009, available at http://www.geosociety.org/science/timescale/timescl.pdf). Key for abbreviations: MORB: mid-oceanic ridge basalt, N-MORB: normal (Atlantic) MORB; E-MORB: enriched (or undepleted) MORB; OIB: oceanic island basalt; BABB: back-arc basin basalt; IAT: island arc tholeiite; REE: rare earth elements; LREE: light REE; MREE: medium REE; HREE: heavy REE; LILE: large ion lithophile element; HFSE: high field strength element.

2. Geologic Outline

[7] The subduction/obduction complex of New Caledonia is composed of four units.

[8] 1. A complex Permian-Early Cretaceous volcano-sedimentary "basement" and its Late Cretaceous to Eocene unconformable sedimentary cover. To the north of the island, this set is involved in the Eocene HP-LT metamorphic complex where it is referred to as the Diahot Terrane.

[9] 2. A mafic/ultramafic metamorphosed mélange (the Pouebo terrane) formed of mafic eclogite facies rocks imbedded in a meta-serpentinite matrix and minor metasediments. Mafic eclogites have Late Cretaceous to Eocene protoliths derived from the Poya Terrane [*Cluzel et al.*, 1994, 2001; *Spandler et al.*, 2005].

[10] 3. A Late Cretaceous to Paleocene mafic allochthon, the Poya Terrane [*Cluzel et al.*, 1997, 2001], composed of sliced oceanic crust rocks and bathyal sediments.

[11] 4. A pre-Eocene ultramafic allochthon, the Peridotite Nappe, mainly formed of upper mantle rocks [*Avias*, 1967; *Collot et al.*, 1987; *Prinzhoffer*, 1981].

[12] Pre-Late Cretaceous rocks comprise three terranes: (1) the Central Chain Terrane containing Permian-Early Cretaceous volcano-sedimentary fore-arc complex composed of Triassic to Early Cretaceous deep-water turbidites deposited on an early Permian ophiolite [*Meffre et al.*, 1996; *Aitchison et al.*, 1998]; (2) the Teremba Terrane, containing Late Permian to Jurassic volcanic-arc rocks [*Cluzel and Meffre*, 2002] with no known basement; and (3) the Boghen Terrane containing a Jurassic(?)–Early Cretaceous accretionary complex, forms the central part of the island; it has been metamorphosed into the blueschist facies in the Early Cretaceous and exhumed before the Late Cretaceous.

[13] These terranes amalgamated after ~95 Ma (age of the youngest volcaniclastic arc turbidite) and before the Coniacian (~89 Ma) on the Australian active margin [*Cluzel et al.*, 2010]. The three pre-Late Cretaceous terranes are overlain by unconformable Upper Cretaceous (Coniacian-Maastrichtian) shallow marine clastic deposits which are, in turn, overlain by conformable Paleocene and Eocene hemipelagic and pelagic chert and micrite, which record the rifting and subsequent thermal subsidence of the Australian margin [*Aitchison et al.*, 1995a]. Unconformable shallow water limestones, mid-Eocene in the middle of the island [*Maurizot*, 2011] and Late Eocene in the south [*Cluzel et al.*, 1998] record a period of emersion due to the passage over a fore-arc bulge [*Cluzel et al.*, 2001] and initiate a prominent change from a stable intraoceanic plateau setting into a mobile foreland basin. The accumulation of 3 to 5 km thick, coarsening upwards turbidites (Bourail Flysch) that overlie the shallow water limestone record an increasing instability and changing sedimentary provenance. The input of coarsening upwards clastic material climaxed with an olistostrome, which contains both sedimentary rock boulders coming from the autochthonous sedimentary cover itself, and mafic rocks from the Poya Terrane as well. As the Eocene unconformity is getting younger southward, it appears that this clastic sequence records the in-sequence southward imbricate thrusting (duplexing) of the sedimentary cover and out-of-sequence overthrusting of the mafic Poya Terrane (see below) that finally overlies the olistostrome itself.

[14] The HP-LT metamorphic complex in the north comprises the metamorphic Diahot and Pouebo terranes (Figures 1 and 2a). The Diahot Terrane rocks do not greatly differ from the Cretaceous-Eocene sedimentary cover, with a more distal character during the Late Cretaceous though and a much higher metamorphic grade (blueschist and eclogite). It shows the same Tertiary sedimentary sequence except the Eocene turbidite-olistostrome dominantly composed of breccias, which started earlier than in the south (Late Ypresian; ~50 Ma) [*Maurizot*, 2011], and characteristically does not contain any mafic rock. The Pouebo Terrane is a subduction melange composed of meter to 100 m scale boulders of mafic rocks coming from the Poya Terrane [*Cluzel et al.*, 2001; *Spandler et al.*, 2005], embedded in a meta-serpentine matrix (talc-schist) and minor metasedimentary rocks. The Diahot Terrane rocks have been subducted at depth ~50 km (1.7 GPa, 550°C) [*Fitzherbert et al.*, 2003, 2005] while eclogites in the Pouebo Terrane have metamorphic mineral associations which suggest a much higher grade and maximum depth of ~80 km (2.4 GPa, 650°C) [*Clarke et al.*, 1997, *Carson et al.*, 1999, 2000]. At present, the Pouebo Terrane, which was subducted at greater depth, appears in the core of a regional-scale antiform wrapped by the Diahot Terrane (Figure 2a). Although no direct contact is visible in the field, and in spite of prominent tectonic complexity, geophysical evidence [*Collot et al.*, 1987] shows that the antiformal structure is in turn overlain by slices of the Poya Terrane and finally by the Peridotite Nappe, which is rooted in the Loyalty Basin (Figures 2a and 2b). The regional-scale antiformal structure of the metamorphic complex may be due either to a late folding of the tectonic pile; or alternatively, to the exhumation of high grade eclogitized melange (Pouebo Terrane) that dragged the overlying rocks (Diahot Terrane) toward the surface.

[15] The Poya Terrane is an allochthonous set of meter to kilometer-scale upright tectonic slices of pillow and massive basalt (~99% of the terrane) associated with thin inliers of bathyal argillite and chert; it is always located below the Peridotite Nappe (Figures 1 and 2). The main body of this unit is located along the west coast where it is 10 km wide on average and extends over ~250 km from Bourail to Koumac; smaller and less continuous units are located along the east coast (Figure 1).

[16] The Poya Terrane basalts are generally unmetamorphosed and do not display any ductile deformation. The local occurrence of lower greenschist or zeolite facies mineral associations is likely due to intraoceanic water-rock interaction referred to as ocean floor metamorphism [*Nicholson et al.*, 2000]. Based upon geochemical features, Poya Terrane basalts form two sub-sets that are undistinguishable in the field; the

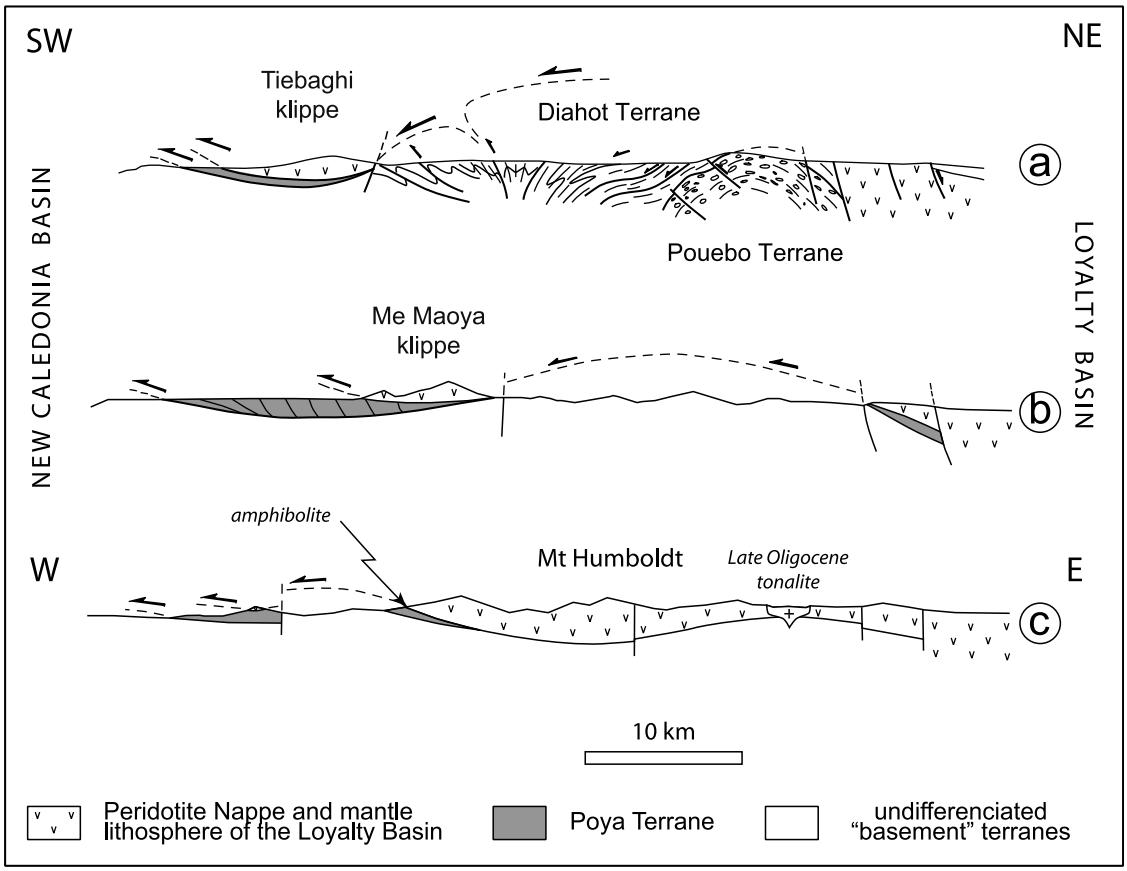

Figure 2. (a) Simplified cross section of the HP-LT metamorphic complex, to show the antiformal structure of the Pouebo Terrane; note that elements of the Poya Terrane and Peridotite Nappe are pinched between the Diahot Terrane and its parautochthonous basement (located to the north of this section) (b) Cross section of New Caledonia at midlatitude to show the geometrical relationship of allochthonous terranes (Poya Terrane and Peridotite Nappe). Note that the undeformed Peridotite Nappe always structurally overlies the tectonically complex Poya Terrane. (c) Cross section of the northern part of the Mt Humboldt Massif, the largest ultramafic unit of New Caledonia, to show the broad open folds that affect the Peridotite Nappe and location of location 4 amphibolites.

largest one (~90%) is composed of undepleted MORB (E-MORB) associated with red bathyal argillite and chert. Bathyal sediments contain radiolarians that assign a Campanian to Upper Paleocene or Lower Eocene age to the bulk of Poya Terrane basalt [*Aitchison et al.*, 1995b; *Cluzel et al.*, 2001]. The smaller one is composed of OIB, and BABB [*Cluzel et al.*, 1994, 1997, 2001; *Eissen et al.*, 1998; *Audet*, 2008] that mainly crop out along the east coast near Thio, and along the west coast near Koné. Both are also composed of fault-bounded slices hundreds of meters long. Alkaline pillow basalts (OIB) contain calcite-filled gas vesicles, are associated with hyaloclastite and pillow breccia, and commonly show rubefaction, a feature consistent with relatively shallow submarine eruption. Both OIB and BABB near Koné display carbonated interpillow material (pink and white micrite respectively) instead of bathyal argillite, and thus indicate eruption depth above the CCD. In the Foué peninsula, the pink micrite beds that overlie pillow lavas of BABB affinity contain planktonic foraminifers that range in age from the Paleocene to the mid- to Late Eocene. At Gatope (near Voh) micrite interpillows similarly display a Paleocene- Eocene microfauna (M. D. Courme, unpublished data, 2008). Especially, the occurrence of *Subbotina triloculinoides* is diagnostic of the transition between the Danian and Selandian (~62 Ma) [*Berggren and Pearson*, 2005; *Berggren et al.*, 1995]. Thus, based upon micropaleontological data of the Poya Terrane rocks, eruption of BABB probably took place during the (lower Middle?) Paleocene while pelagic sedimentation continued at least until the mid-Eocene. However, undated BABBs without carbonate interpillows crop out along the east coast (near Thio, Figure 1) [*Cluzel et al.*, 2001], and new U-Pb on zircon data (this study) indicate that BABB emplacement may also have taken place as soon as Early Maastrichtian time (~70 Ma; see section 7.2).

[17] These slices of upper oceanic crust have been peeled off from the lower plate of the subduction complex (the South Loyalty Basin), and accreted to the Eocene fore-arc. The Poya Terrane was thrust upon New Caledonia during the Late Eocene as recorded by the arrival of coarsening upwards mafic detritus in foreland basins (for details regarding the Poya Terrane, see *Cluzel et al.* [2001]). It is worth noting that meantime, the Peridotite Nappe was not in

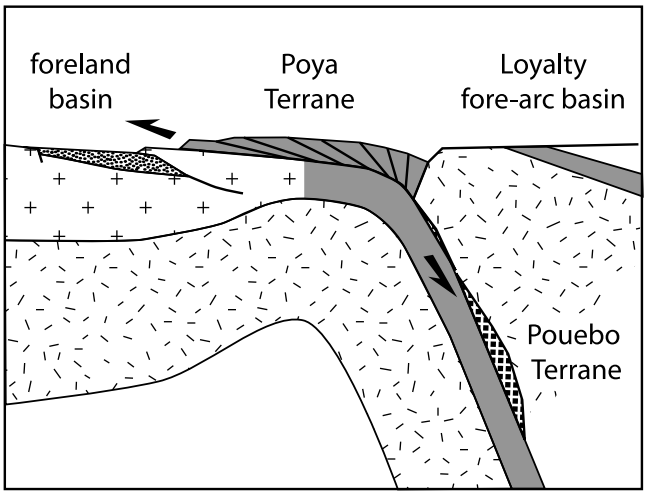

Figure 3. Sketch diagram of the Eocene subduction (no scale) to show the formation of the cordilleran Poya Terrane by peeling off the lower plate and the coeval emplacement of Pouebo eclogitized melange with the same origin at depth (for clarity, the Diahot Terrane has not been represented).

a position to feed the basins because no peridotite-derived clasts (chromite, orthopyroxene or serpentine) are present (Figure 3).

[18] Mafic eclogite-facies boulders in the Pouebo Terrane have the same geochemical features as Poya Terrane basalts (E-MORB), 85–55 Ma U-Pb magmatic zircon ages, and therefore likely originated from the same upper oceanic crust unit (Figure 3) [*Cluzel et al.*, 2001; *Spandler et al.*, 2005]. Mid-Eocene U-Pb zircon overgrowth ages (~44 Ma) in eclogite [*Spandler et al.*, 2005] show that peak metamorphism (i.e., exhumation inception) of the Pouebo Terrane occurred 6 Ma after beginning of tectonism in the northern part of the foreland basin (~50 Ma) [*Maurizot*, 2011]. The syn-sedimentary tectonic activity was likely due to the imbricate thrusting of the Upper Cretaceous-Paleocene sedimentary cover when the Norfolk ridge started jamming the subduction zone and eventually resulted in inception of exhumation. Exhumation of eclogite was almost completed at ~34 ± 4 Ma (apatite fission tracks) [*Baldwin et al.*, 2007], while the youngest pre-obduction autochthonous sediments were being deposited (Formation de la Cathédrale; Late Priabonian, 35.0–33.7 Ma) [*Cluzel et al.*, 1998]. These time constraints show that there is a close genetic relationship between subduction and obduction, while high-grade metamorphic rocks were exhumed from beneath the ultramafic allochthon (i.e., the fore-arc mantle) during, or immediately after its final tectonic emplacement.

[19] The ultramafic Peridotite Nappe is dominantly formed of upper mantle rocks (harzburgite and rare lherzolite) with minor ultramafic (pyroxenite, wehrlite and dunite) and mafic (layered gabbro) cumulates [*Prinzhoffer*, 1981]. These ultramafic rocks reflect a complex history that include several stages of melting, rock-melt interaction, and re-melting [*Marchesi et al.*, 2009; *Ulrich et al.*, 2010] that finally lead to an extreme overall depletion.

[20] The base of the ultramafic allochthon is formed of 20 to 100 m thick porphyroclastic serpentine mylonite that likely formed during obduction and locally indicates southwest-directed shearing. In general, the Peridotite Nappe lies undeformed above a sub-horizontal fault (Figure 2b), with the very simple structure sharply contrasting with the complexity of underlying terranes and especially the Poya Terrane.

[21] The Peridotite Nappe is crosscut at all levels by Early Eocene ultramafic-mafic (hornblendite to micro-diorite), and felsic (leucodiorite to granite) coarse grain dykes intruded in a very narrow span of time (53.1 ± 1.6 Ma - 49.6 ± 2.8 Ma; U-Pb on zircon; mean = 53.0 ± 0.3 Ma on 7 samples) [*Cluzel et al.*, 2006]. Basalt (dolerite) dykes also appear in about the same setting but are not well time-constrained because they do not contain zircon; a poorly defined whole rock K-Ar age at ~50 Ma [*Prinzhoffer*, 1981] is of questionable reliability.

[22] It is worth noting that early Eocene pre-obduction dykes are unmetamorphosed and do not display any deformation except when they are located in the mylonitic serpentinite sole of the peridotite Nappe, where they are fractured and fragmented. The only exception comes from certain diorite or hornblendite dykes that display some internal ductile deformation features (boudinage and preferred orientation of amphibole, and locally microfolding), while dyke walls remain planar. These features suggest that shearing occurred during or immediately after magma injection in moderately active faults.

[23] Dolerite dykes are dominantly IAT-like and therefore have been formed in a supra-subduction setting. Micro-diorite and hornblendite result from hydrous melting of a similar supra-subduction source; while in contrast, most felsic dykes display the geochemical features of slab melts [*Cluzel et al.*, 2006]. Thus, a transient high-temperature gradient in the fore-arc region during earliest Eocene time probably generated this short-lived magmatic event with arc and fore-arc magmatic affinities.

[24] In summary, the "ophiolitic" complex of New Caledonia is formed of superposed mafic and ultramafic allochthons, which correspond to the Cordilleran (accretionary) and Tethyan (collisional) types respectively [*Dilek*, 2003]. The allochthonous terranes are associated with a subduction complex formed of metamorphosed (HP-LT) rocks and syntectonic foreland sedimentary basins. This association tightly constrains its geodynamic setting and tectonic emplacement processes.

3. Geometrical Relationship Between Mafic/Ultramafic Allochthons and the HP-LT Complex

[25] There is little contact between HP-LT metamorphic rocks and the mafic/ultramafic allochthons because syn- and post-exhumation erosion has removed the bulk of overlying (upper plate) units. It is clear however that the Peridotite Nappe and to a lesser degree, the Poya Terrane overlie the lower grade (external) part of the HP-LT complex. This relationship may be observed in the north of the island and along the east coast, where southwest verging tight folds (Koumac) and shallow east-dipping foliation (Houailou) pass below the basal thrust of the Peridotite Nappe and below Poya Terrane basalts as well. Along the east coast, between Hienghène and Houailou, lenses of Poya Terrane basalts are pinched between the HP-LT schists and the peridotites that form the basement of the lagoon (see below). However, in the rest of the island, high grade HP-LT rocks

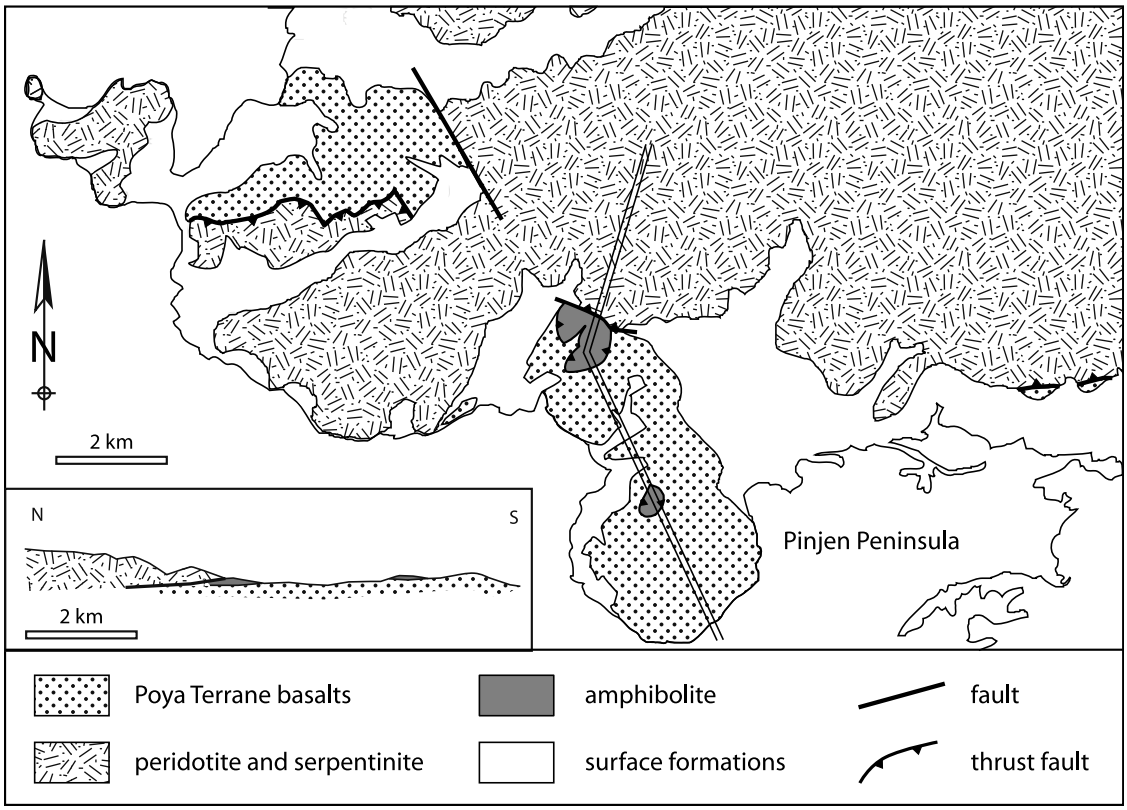

Figure 4. Geological map and cross section of the Pinjen peninsula area (location 1 in Figure 1).

are never located at the base of the mafic or ultramafic allochthons. An elongate positive gravity anomaly (+150 mGal) located along the east coast suggest that peridotites are hidden below the eastern lagoon, a feature that infers that the Peridotite Nappe is rooted in the Loyalty Basin [*Collot et al.*, 1987], and separated from autochthonous units by a large normal (?) fault, almost 400 km long (Figure 2).

[26] Thus, the relationship between HP-LT rocks and the mafic-ultramafic allochthons has exclusively a tectonic character; therefore, in contrast with amphibolites that are located immediately below peridotites (see section 4), a metamorphic sole setting cannot be advocated for the Eocene HP-LT rocks. In addition, there are large differences of crystallization timing between amphibolites (~56 Ma, see section 7) and eclogites (44 and 38 Ma, respectively).

4. Location and Features of Amphibolite Lenses

[27] Amphibolites crop out in four localities: (1) Pinjen Peninsula near Koné, (2) Mueo Pass near Népoui, (3) Petchecara Pass near Thio, and (4) in the Upper Ouenghi watershed, along a small tributary of the Wa Kwèja (river), 13 km to the east of Bouloupari (locations shown in Figure 1).

[28] In three of these localities (1, 2, and 3), amphibolite lenses are clearly located below the serpentinite sole of the Peridotite Nappe, above Poya Terrane basalt, and except at Muéo Pass, the tectonic boundaries are rather simple and shallow dipping. In addition, strongly weathered meter-size boulders of amphibolite also crop out within serpentine mylonite along the right (western) bank of the Nepoui River; but their geometrical relationships are far from clear. More occurrences are likely, but owing to the deep weathering and bad outcrop conditions of the west coast, they have remained unnoticed.

[29] Pinjen amphibolite (location 1 in Figure 1), wrongly referred to as "diorite" on the 1/50,000 geological map, Pouembout sheet [*Carroué*, 1972], appears in two masses that probably formed originally one single large lens (Figure 4). The larger one is located in a small quarry to the north of the main RT1 road; it extends approximately over 600 × 750 m and is ~10 m thick. A smaller outcrop may be seen along road cuts of the RT1 at ~300 m to the east of the quarry; the second one (300 × 500 m) crops out in a small hill below a water tank at ~1 km to the SSW of Pinjen Station. Pinjen amphibolite displays a prominent textural zoning from a schistose and fine-grained cortex toward a coarser grained and ribbon-textured nucleus. On top of the lens, the foliation is shallow dipping and is parallel to the boundary with serpentine, while it dips 50° at Pinjen Hill that probably represents the innermost part of the lens; a geometrical feature consistent with an internal rotation due to southwest-directed tectonic emplacement. Pinjen amphibolite is composed of hornblende, clinopyroxene, two generations of plagioclase (high-Ca and low-Ca), magnetite and sphene (titanite) cored by ilmenite.

[30] The tectonic boundary with the underlying Poya Terrane basalt does not crop out, but the lens has been core-drilled for water exploration near Pinjen Hill. The basal part of the amphibolite lens is formed of cataclasite crosscut by an anastomosed fracture set filled with crushed material. Low-temperature minerals such as poorly crystallized chlorite, zeolite, and opaque minerals fill-in sinuous fractures

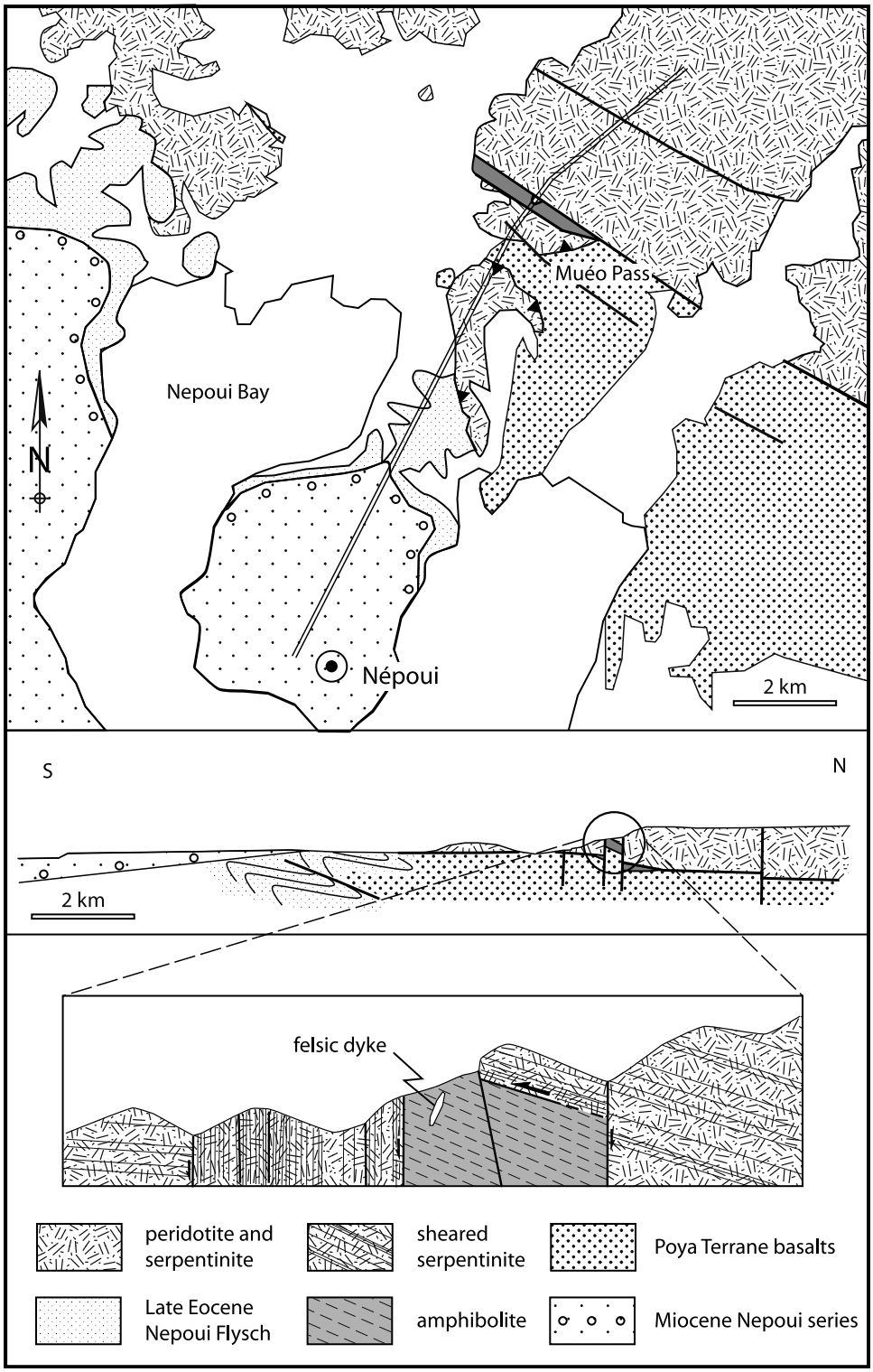

Figure 5. Geological map and cross section of the Mueo Peninsula area (Nepoui) (location 2 in Figure 1).

and infer low temperature conditions during the final tectonic emplacement of amphibolite. The underlying Poya basalt is unmetamorphosed reddish vesicular basalt that closely resembles Paleocene OIB of the same locality.

[31] At Muéo Pass (Nepoui, location 2 in Figure 1) a well-layered amphibolite body about 50 m thick, crops out in a narrow horst bound by steeply dipping normal faults that crosscut the basal serpentinite sole (Figure 5). Amphibolite foliation dips 20° to the north and is conformable with the basal contact of serpentinite. The rock is composed of dark brown hornblende, clinopyroxene, plagioclase, and magnetite.

[32] Two light colored dykes one meter long and 10–15 cm thick crosscut the amphibolite obliquely; they apparently lack foliation, but display zigzag boundaries due to intrafolial slip of the amphibolite and therefore they have probably been deformed together. These dykes are composed of hypersthene, alkali feldspar and sphene; a paragenesis which likely records relatively high metamorphic temperatures.

[33] In a small quarry a few meters below the base of the main lens, amphibolite boulders a few meters in size are enclosed within the serpentine mylonite about 50 m thick, that forms the tectonic sole of the Peridotite Nappe. The rock is dark gray and looks massive on the outcrop, but it is actually a porphyroclastic mylonite composed of amphibolite clasts surrounded by anastomosed ribbons of fine-grained cataclasite. Rock clasts contain hornblende, epidote, and rare albite as a "primary" phase.

[34] On the eastern side of Petchecara Pass, along the road track between Thio and Canala (location 3 in Figure 1), a 50 m long, 10 m thick amphibolite body crops out immediately below the serpentinized tectonic sole of the ultramafic allochthon. It is a gray-green massive rock with some layering though. It is composed of fine to medium grain brown-green hornblende, albite, epidote and sphene, secondary light-green actinolite needles and chlorite flakes. Thin epidote and epidote-actinolite veins also crosscut the rock.

[35] Amphibolites of the location 4 (Ouenghi) do not croup out, but very fresh decimeter- to meter-size dark angular boulders are found mixed with peridotite pebbles along a small tributary of the Wa Kwèja (river) that steeply flows across the base of the Peridotite Nappe with Poya Terrane outcrops found downstream. No amphibolite boulders have been found upstream the base of the Peridotite Nappe; therefore, this amphibolite lens, similarly to other localities, is pinched below the peridotites and above Poya Terrane basalts. Amphibolites of that locality are generally fine grained and well foliated, and some samples show a well defined mineral/stretching lineation marked by aligned hornblende needles; sparse amphibolite cataclasite boulders probably come from to the base of the lens. Therefore, rocks of this locality although they do not crop out, display the same general features as the other amphibolite lenses. In addition to amphibolite boulders, centimeter to decimeter-size flat quartz-rich schist pebbles appear along the stream. One of these pebbles is formed of associated amphibolite and quartz schist. It is likely that quartz-schist although strongly recrystallized and sheared may be a meta-chert. This feature is important because it suggests that amphibolite protoliths were probably oceanic crust rocks.

[36] There is no evidence for amphibolite partial melting in any of the four localities, a fact that is corroborated by the temperature-pressure constraints (see section 6), which are within uncertainty, slightly below the wet solidus of basalt (depending upon partial water pressure) [*Peacock et al.*, 1994; *Poli*, 1993]. In all known occurrences, the amphibolites rest below the serpentinite sole of the Peridotite Nappe and above unmetamorphosed Poya terrane basalts, with cataclasite at the base. The internal foliation generally dips gently and is conformable with tectonic boundaries. These features suggest that amphibolites have crystallized at depth and thereafter have been transported onto the Poya Terrane in a much cooler thermal regime. Probable metamorphosed abyssal sediments were found in one single locality only; however, this is a crucial point that suggests that the protoliths of these metamorphic rocks probably originated in an oceanic crust setting, a hypothesis supported by geochemical data (see section 6). It is worth noting that abyssal sediments are rare in the Poya Terrane, the most probable origin of amphibolites (see below).

5. Pressure-Temperature Constraints

[37] A precise thermo-barometric study of these metamorphic rocks is beyond the scope of this article; however, a rough evaluation of the peak metamorphic conditions is necessary for understanding the overall tectonic setting of amphibolites. Therefore, an attempt has been made to evaluate pressures and temperatures of recrystallization based upon a limited amount of mineral compositions obtained by electron microprobe analysis (for details on analytical procedures see the auxiliary material).[1]

[38] Each of the four localities apparently displays a different metamorphic grade. The Nepoui amphibolite is formed of an association of clinopyroxene, brown hornblende, plagioclase, and magnetite. At Pinjen, amphibolites contain a primary association of plagioclase, brown-green hornblende, epidote, ilmenite and sphene. Petchecara amphibolites contain hornblende, albite, epidote and sphene. Actually, these mineral associations are not all consistent with the P-T estimates provided by mineral compositions and geothermobarometry (see below); therefore, they probably record various stages of retrogression rather than peak metamorphic grade. This view is confirmed by textural relationships; the core regions of incompletely retrogressed amphiboles typically display the highest Ti and Al contents; while low Ca rims generally appear around plagioclase. Titaniferous minerals are generally ilmenite rimed by titanite (sphene). In the following section, most analyses have been selected for evaluating the peak metamorphic conditions and thus a limited amount of data is available only.

[39] Most amphiboles in the three localities have compositions close to the tschermakite-pargasite boundary; however, actinolites or high-Si edenites are probably low grade pseudomorphs of tschermakite-pargasite. Amphibole compositions apparently define a rectilinear compositional trend that may be related to retrogression during cooling in presence of excess water (Figure 6; see also Table S1 in the auxiliary material).

[40] Temperature evaluation has been attempted by using the empirical Ti-in-hornblende geothermometer of *Otten* [1984] that provided a temperature range of 725 to 835°C, and the geothermobarometer of *Ernst and Liu* [1998] that provide a temperature range of 800–900°C and pressures ~0.5 GPa. Significantly higher temperatures (864 to 984°C) have been estimated using the hornblende-plagioclase geothermometer of *Holland and Blundy* [1994] modified by *Anderson and Smith* [1995] (Table S2).

[41] The Al-in-hornblende barometer [*Schmidt*, 1992] is based upon the bulk Al content of the hornblende cell, which

[1] Auxiliary materials are available in the HTML. doi:10.1029/2011TC003085.

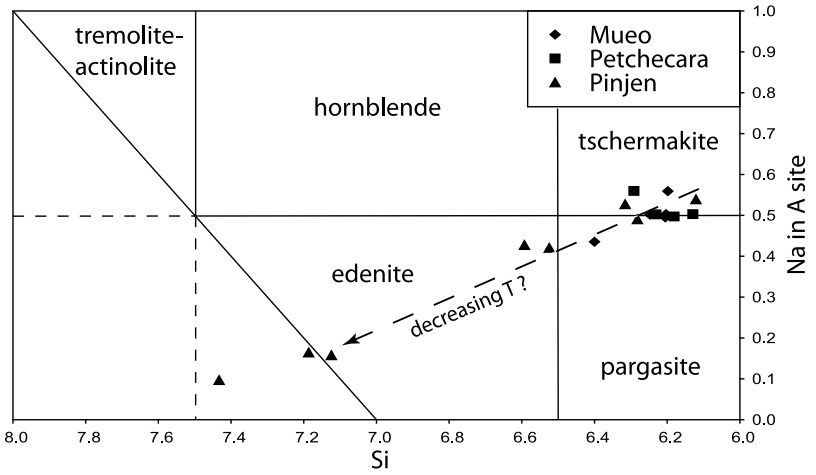

Figure 6. Classification of amphiboles after *Leake et al.* [1997]; note the large compositional range of amphiboles from the Pinjen site that possibly depict pseudomorphic high grade amphibole replacement by edenite/actinolite during amphibolite cooling in presence of excess water ("hydrothermal" recrystallization).

is thought to be controlled by pressure; however, it may only provide a rough estimate of amphibolite crystallization pressure because Al content in hornblende is also controlled by bulk rock chemistry and occurrence of other Al-bearing mineral phases. The average pressures obtained on the three sites by this method vary from 0.44 to 0.52 GPa (Table S2). Pressure estimate may also vary depending upon temperature; based upon temperatures evaluated by the hornblende-plagioclase geothermometer (see above) [*Anderson and Smith*, 1995] corrected pressures vary from 0.47 to 0.50 GPa (Table S2). The absence of garnet and conversely, occurrence of ilmenite and sphene instead of rutile are consistent with this moderate pressure range.

[42] The application of the Ti-Al-in-hornblende geothermobarometer of *Ernst and Liu* [1998] does not greatly improve the P-T evaluation. The peak P-T conditions estimated by this method (850°C, 0.45 GPa; Figure 7), are consistent with the results above; however, the main difference comes from lower temperature results that indicate a pressure up to 1 GPa at ~750°C (Table S2). Although this result should be taken with much care, it may indicate cooling at increasing pressure.

[43] Thin epidote, epidote-actinolite, and prehnite veins also commonly crosscut the amphibolites, depending upon rock composition. Secondary actinolite or tremolite needles, and chlorite flakes form a greenschist-facies retrograde association caused by subsequent cooling. The low-grade cataclasite at the base of the unit probably formed during the final tectonic emplacement in relatively shallow low-grade conditions.

6. Geochemistry

[44] Outcrop conditions along the west coast low lands of New Caledonia are generally very bad and owing to the prominent weathering that prevails, only a few relatively fresh samples could be collected and analyzed. However, only limited geochemical variability appears in the data set, and the analyses presented below should be considered as representative. Although they are completely recrystallized and generally display rare magmatic mineral relicts only (clinopyroxene), the amphibolites most probably derive from mafic magmatic rocks. Amphibolites are basaltic in terms of Al_2O_3 contents (Al_2O_3 = 11–16 wt %), although their SiO_2 content vary from 43 to 56 wt %. Since syn-metamorphic mobility is generally low in high grade metamorphic rocks [*Ghatak et al.*, 2012], variation in mobile elements contents (Si, Na, K, Ca, Rb, Ba, Sr,..) and high H_2O contents (LOI = 1.5–3.5 wt %) are probably a consequence of moderate weathering which is apparent in the field; or alternatively, of ocean floor metamorphism (pre-amphibolitisation) that affected the protolith [*Cluzel et al.*, 2001]. Therefore, major element compositions cannot be used for rock classification. Instead, trace elements ratios and chondrite-normalized REE patterns [*Evensen et al.*, 1978; *Pearce*, 1982], less sensitive to fluid-driven elemental fractionation, are used for rock discrimination. The Zr/TiO_2

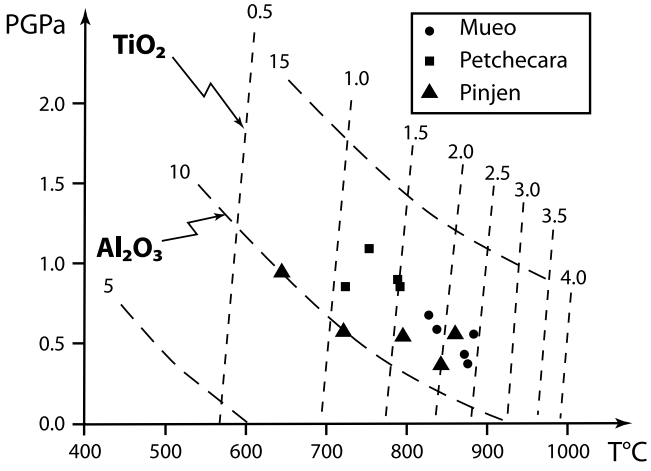

Figure 7. An estimation of pressure and temperature using the geothermobarometer of *Ernst and Liu* [1998]. Values associated to the TiO_2 and Al_2O_3 isopleths are in wt%. Note the increasing pressure associated with decreasing temperature for Pinjen amphiboles (see also Figure 6).

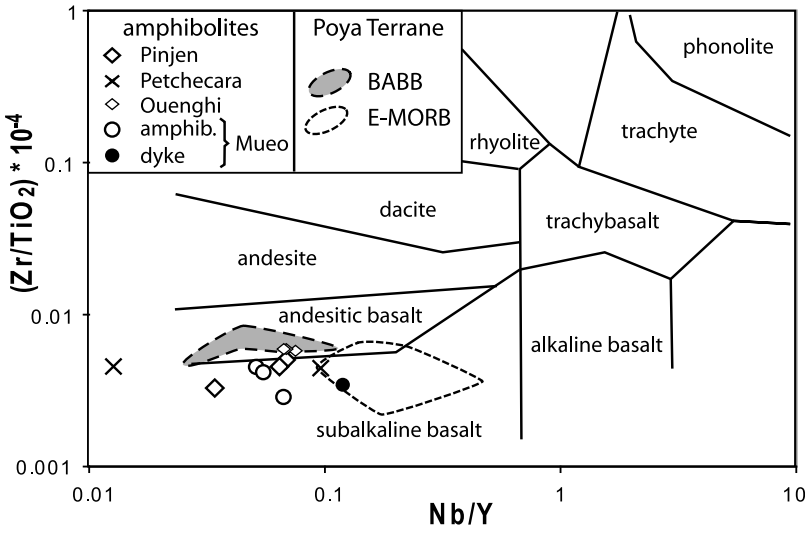

Figure 8. Zr/TiO_2 versus Nb/Y classification diagram of *Winchester and Floyd* [1977]. All amphibolites plot in the subalkaline basalt field. Note that the very low value of the Nb/Y ratio for BCE6b is probably due to an under evaluated Nb content (Nb = 0.15 ppm; Table S3). In terms of Nb/Y ratio, amphibolites bear the closest similarity with the BABB of the Poya Terrane although their Zr/TiO_2 ration is slightly lower. Delineated fields for Poya Terrane basalts are based upon 77 samples (11 BABB and 66 E-MORB) [*Cluzel et al.*, 2001].

versus Y/Nb diagram of *Winchester and Floyd* [1977] (Figure 8), is currently used instead of the classical TAS diagram [*Le Bas et al.*, 1986]. On this diagram, the amphibolites mainly plot within the subalkaline basalt field.TiO_2 contents are low (TiO_2 = 0.4–1.25 wt %) and consistent with subalkaline basalt series, except for one sample (Pb50135–6; TiO_2 = 3.4 wt %), which also displays a much higher Fe content (20 wt %).

[45] Based upon normalized REE patterns (Figure 9), two types may be distinguished: (1) LREE-depleted and (2) REE-depleted. The type 1 is found at Pinjen (3 samples), at Nepoui (3 samples), at Ouenghi (3 samples), and also at Petchecara Pass (1 sample). The rocks are depleted in LREE ($0.36 < (La/Sm)n < 0.67$) with a flat MREE and HREE distribution and thus resemble to mid-oceanic ridge basalt (MORB) (http://www.petdb.org) [*Lehnert et al.*, 2000]. They contain the same bulk amount of REE than an average MORB [*Sun and McDonough*, 1989] and thus are likely to result from a similar amount of fractional melting of a depleted mantle source. The REE-rich sample (Pinjen) displays a weak Eu negative anomaly, which is consistent with fractional crystallization of plagioclase, and could be a differentiation product of the same magma. However, low SiO_2 (42 wt %) and Al_2O_3 (11.6 wt %), high FeO (20 wt %) and high TiO_2 (3.30 wt %) contents are inconsistent with this interpretation, and may be plausibly related to a higher amphibole content due to metamorphic layering.

[46] On the REE and trace elements expanded spider diagram normalized to the average N-MORB [*Sun and McDonough*, 1989] (Figure 10), the type 1 amphibolites display a weak negative Nb anomaly. Nb depletion in a mafic rock is generally ascribed to partial melts from mantle that contains Nb-retaining refractory mineral phases such as pargasite [*Tiepolo et al.*, 2000], or spinel [*Bodinier et al.*, 1996], a feature of volcanic-arc magma sources. However, there is no noticeable Ta anomaly with respect to La; and $(Nb/Ta)_n$ is constantly less than 1. A very low Th content (0.03–0.15 ppm) is also a common feature of type 1 amphibolites. In addition, the Ti negative anomaly that appears in most subduction-related magmas because of residual Ti oxide [*Kalfoun et al.*, 2002] is absent. Such signatures suggest weakly metasomatized or mixed supra-subduction mantle source containing a small amount of a low-Ti amphibole. There is also bulk enrichment in LILE (Ba, Rb, K; 2 to 10 times MORB concentrations)

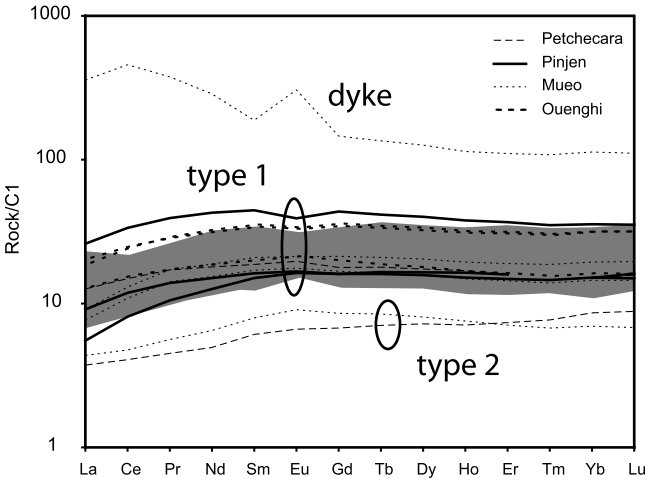

Figure 9. A comparison of the geochemical features of amphibolites and their possible protoliths. Chondrite-normalized REE patterns of Early Eocene amphibolites after *Pearce* [1982, 1996] (Table S3), compared with the compositional field of BABB of the Poya Terrane (shaded). The data for the BABB-type of Poya Terrane basalt (24 samples in all) is from *Cluzel et al.* [2001] and *Audet* [2008]. The normalization value (C1) is from *Evensen et al.* [1978].

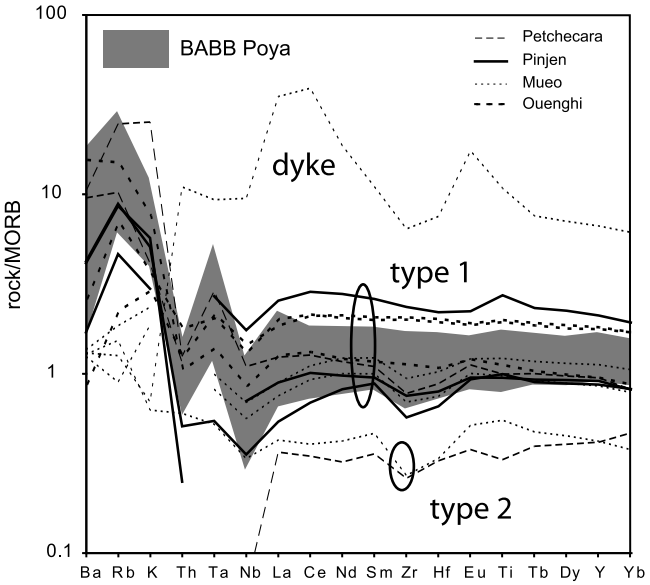

Figure 10. Rare earth and trace elements expanded spider diagram normalized to the average MORB [after *Sun and McDonough*, 1989]. The shaded area depicts the compositional field of BABBs of the Poya Terrane. Data has the same provenance as Figure 9.

(Figure 10), which is generally interpreted as a subduction-related feature; i.e., source enrichment from slab-derived fluids, or preferential LILE extraction during hydrous melting. However, even if in most high-grade metamorphic rocks, the bulk chemical composition remains almost unchanged except for some LILE [*Spandler et al.*, 2004; *Ghatak et al.*, 2012], during low and medium grade metamorphic events, hydrous fluid ingress may also result in enrichment in "mobile" incompatible elements, depending upon rock/fluid ratio; therefore, LILE enrichment should be considered with much care. Hence, the type 1 amphibolites are metamorphosed tholeiites, generated by a moderate degree of low pressure fractional melting of a weakly metasomatized mantle source, or a mixture of metasomatized and juvenile sources. Such a process produces magma compositions similar to back-arc basin basalt (BABB), intermediate between IAT and MORB [*Langmuir et al.*, 2006].

[47] The type 2 pattern characteristically display low bulk REE content, and LREE depletion compared to HREE that leads to an overall positive slope (Figure 9). Despite lower REE contents and slightly different REE patterns, such REE-depleted basalts are commonly associated with "normal" MORB (see http://www.petdb.org) [*Lehnert et al.*, 2000] and are likely due to a higher melting degree, or re-melting of a similar mantle source. On the REE-trace elements expanded spider-diagram, the depleted amphibolite-cataclasite Mueo1 shows a weak negative anomaly in Nb, while no Ta anomaly appears (Figure 10) and is thus similar to the type 1. In contrast, the sample BCE6b has an extreme depletion in Nb (0.148 ppm), and its Ta content is below the detection limit (<0.015 ppm) (Table S1), thus depicting an origin from a Nb-Ta-depleted or Nb-Ta-retaining source closer to IAT than to MORB.

[48] Two samples of type 1 amphibolites have been analyzed for Nd and Sr isotopes, their Nd isotopic ratio back-calculated at 60 Ma (postulated age of eruption; see section 2), are within the range of most back-arc basin basalts (εNd = 7.1 and 8.3; Table S4); using a slightly older age (e.g., 80 or 90 Ma) does not change the result significantly. The Sr isotopic ratios higher than that of oceanic rocks (the mantle array), have probably been modified during retrograde low grade metamorphism and/or moderate weathering by radiogenic Sr input.

[49] Although slightly different, the type 1 amphibolites display the closest geochemical similarities with the Paleocene BABB-like rocks of the Poya Terrane that crop out in Foué and Gatope peninsulas (see section 2).

7. Time Constraints

7.1. $^{40}Ar/^{39}Ar$ Hornblende Thermochronology

[50] Dating metamorphic events would require chronologic systems that close within the temperature range of peak metamorphism. In the case of amphibolites, the hornblende K-Ar system closes at a temperature (550 ± 50°C) [*Villa et al.*, 1996], which is well below the temperature range of the amphibolite (850–980°C; see section 4); therefore, the $^{39}Ar^{40}Ar$ apparent age of hornblende only provides an estimate of the cooling age of amphibolite.

[51] The sample studied (PO11B) comes from the Pinjen Peninsula, in the same group of outcrops as PO11 and PO11A. It is representative of the average composition of type 1 amphibolite. This medium-grained amphibolite is composed of aligned fresh hornblende crystals associated with epidote, plagioclase and minor sphene.

7.1.1. Analytical Methods

[52] We separated unaltered, ~250 μm-size, hornblende. These minerals were separated using a Frantz magnetic separator, and then carefully hand-picked under a binocular microscope. The selected hornblende grains were further leached in diluted HF for one minute and then thoroughly rinsed with distilled water in an ultrasonic cleaner. The ages were calculated with the decay constant values of *Renne et al.* [2010] and using Fish Canyon sanidine (FCs) as a neutron fluence monitor for which an age of 28.305 ± 0.036 Ma (1σ) was adopted [*Renne et al.*, 2010], based on the calibration by *Jourdan and Renne* [2007]. Argon isotopic data corrected for blank, mass discrimination and radioactive decay are given in the auxiliary material. All sources of uncertainties are included in the calculation. Detailed analytical procedures are also given in the auxiliary material.

7.1.2. $^{40}Ar/^{39}Ar$ Results

[53] The hornblende sample yields a plateau age of 55.8 ± 1.7 Ma (2σ; MSWD = 0.93; P = 0.54) including 100% of the ^{39}Ar released (Figure 10a). The inverse isochron (Figure 11b) shows an excellent spread along the mixing line and gives an age of 55.4 ± 2.0 Ma (MSWD = 0.99; P = 0.46) similar to the plateau age, and a $^{40}Ar/^{39}Ar$ ratio of 300 ± 7; indistinguishable from the atmospheric ratio of ~298.6. The plateau age of 55.8 ± 1.7 Ma is therefore interpreted to represent the time of closure of hornblende K-Ar system at ~550°C.

7.2. U-Pb Radiochronology of Zircon and Sphene

[54] Zircon is a high temperature, ultra-resistant mineral that generally appears in felsic or intermediate magmatic rocks, more rarely in mafic rocks, or in high grade metamorphic

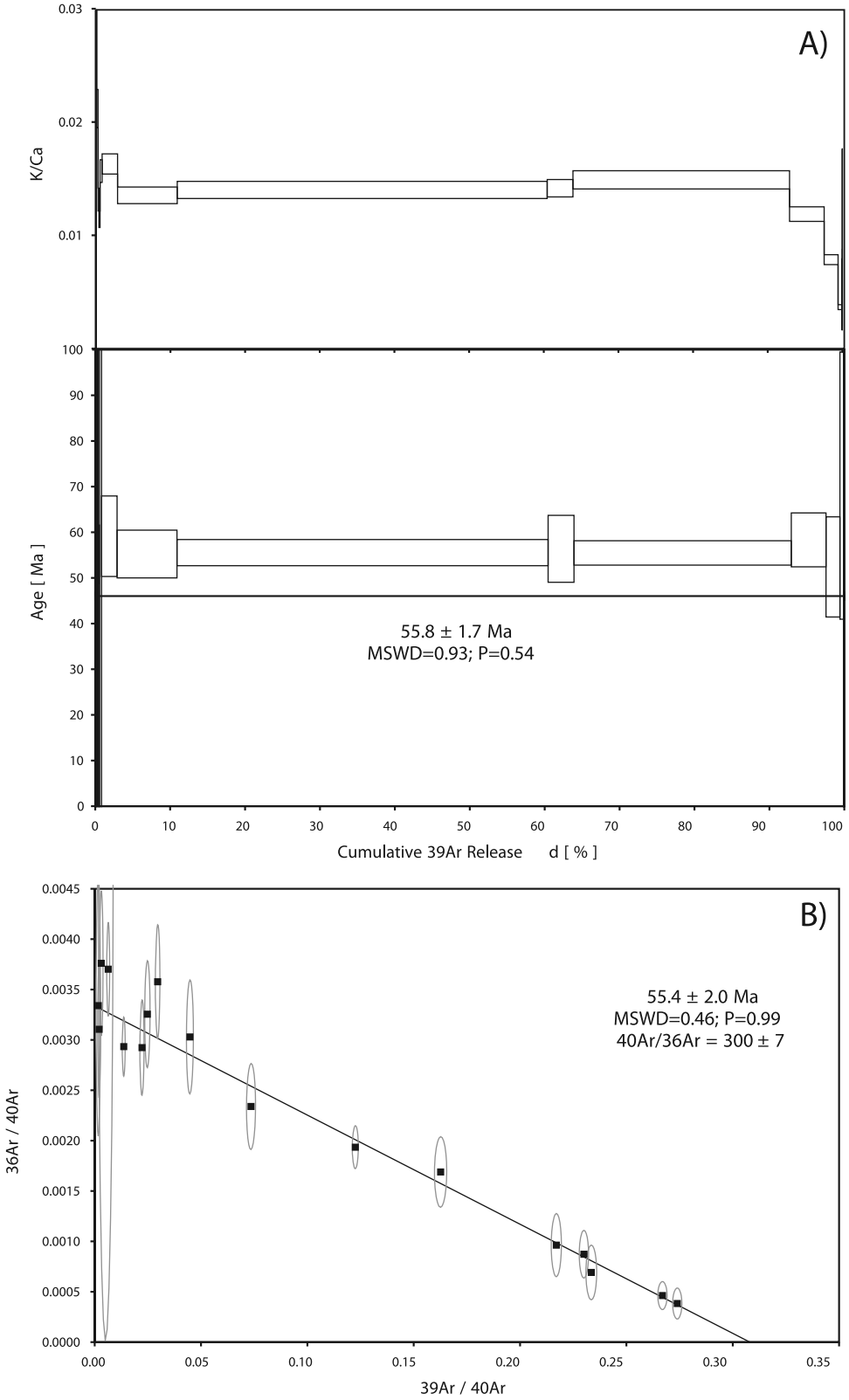

Figure 11. (a) $^{40}Ar/^{39}Ar$ step heating age and K/Ca spectra of hornblende extracted from sample $PO11_B$ (Pinjen Peninsula). (b) Inverse isochron age. Note that the largely invariant K/Ca ratio indicates the absence of compositional zoning and homogeneous behavior of hornblende through the degassing process. All ages are given at 2σ and include all sources of uncertainties.

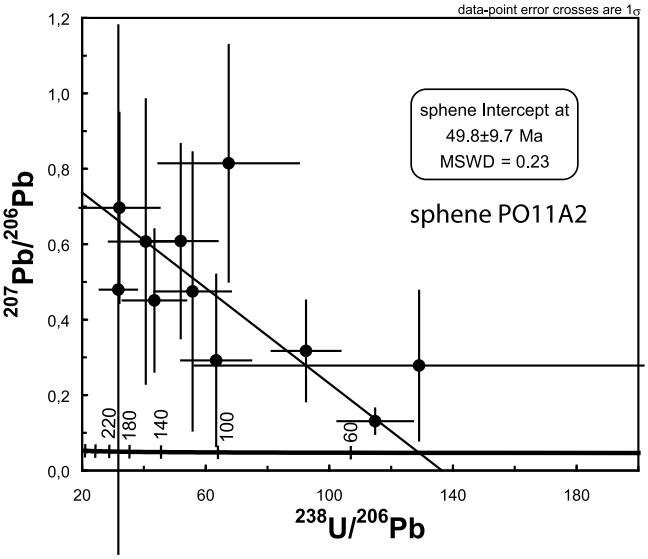

Figure 12. Reverse concordia diagram (Tera–Wasserburg) showing the U/Pb isotopic ratios of sphene analyzed from sample PO11A. The bulk of the data is discordant due to extremely low U (av. 2.8 ppm) and a small amount of common Pb. The 11 sphene grains analyzed allow a poorly defined lower intercept at 49.8 Ma to be computed. (calculated by the isoplot program of *Ludwig* [2003]). Solid line is a mixing isochron through the data anchored common Pb at 49.8 Ma [*Stacey and Kramers*, 1975].

rocks. Zircon generally crystallizes at temperatures above 650 °C, and in high-temperature metamorphosed magmatic rocks, primary zircon generally form the nucleus around which metamorphic zircon overgrowths appear. In this study, only one zircon core is likely magmatic, the rest have most probably a metamorphic origin.

[55] Sphene in metamorphosed mafic rocks comes from the redistribution of Ca and Ti contained in clinopyroxene and plagioclase. At moderate pressure the stability field of sphene is within the range of 400–600 °C depending upon pressure [*Frost et al.*, 2001]; therefore, in amphibolite-facies mafic rocks, it is related to metamorphic recrystallization and there is little chance for its U-Pb system to be inherited from the original magmatic rock. In this article, U-Pb isotopic data from sphene is used to date metamorphic crystallization in an attempt to complement $^{40}Ar/^{39}Ar$ thermo chronological data.

[56] Two amphibolite samples (PO11A2, and BCE6b) and one felsic dyke (Mueo4) that crosscut it have been processed for heavy mineral separation (sphene and zircon) and LA-ICPMS U-Pb geochronology at Hobart University. Only one sample yielded sphene (PO11A), only one contained zircons (Mueo4) and none of the two minerals could be extracted from the third sample (BCE6b)

7.2.1. Pb Geochronology Results

[57] The sample PO11A2 (Pinjen) that yields an $^{40}Ar/^{39}Ar$ apparent age of 55.8 ± 1.7 Ma yields a poorly defined U-Pb age of 49.8 ± 9.7 Ma (2σ; sphene) (Figure 12) as the result of very low U in sphene (2.8 ppm). Within error, the U-Pb age of the sphene is indistinguishable from the hornblende $^{40}Ar/^{39}Ar$ age, but the low precision does not allow drawing further conclusion. Therefore, the hornblende $^{40}Ar/^{39}Ar$ age of ~56 Ma will be preferred in the following discussion.

[58] The sample Mueo4, a hypersthene-feldspar-bearing metamorphosed felsic dyke that crosscuts Muéo (Nepoui) amphibolite, contains zircon crystals that yield a well-defined U-Pb age of 55.9 ± 0.8 Ma (based on 11 zircon grains; Figure 13). The sample Mueo4 also yields one single older grain core (69.8 ± 2.5 Ma), which is probably an inherited magmatic zircon.

[59] The occurrence of a probable inherited magmatic zircon at ~70 Ma (Maastrichtian) in this dyke provides an indirect time constraint on amphibolite protolith which cannot be younger than the crosscutting dyke. Therefore, at variance with micropaleontologic results on Poya Terrane interpillow material (see section 2), it appears that BABBs may have erupted sooner than previously thought [*Cluzel et al.*, 2001] and that BABB eruption probably continued at least from the lower Maastrichtian to the Late Paleocene or Early Eocene.

[60] Considering the estimated high temperature range of Mueo (Nepoui) amphibolite (~900°C; see section 4), magmatic zircons if any, have completely recrystallized, except probably a few inherited cores. Therefore, the U-Pb age at 55.9 ± 0.8 Ma probably represents the timing of peak metamorphism of Mueo (Nepoui) amphibolite.

8. Discussion

[61] Amphibolites that appear at the base of ultramafic allochthons, e.g., in the footwall of a subduction zone, are likely originated in the lower plate of the system; however, comparison with the underlying Poya Terrane MORBs shows some differences. For instance the E-MORB type basalts that represent ~80% of the Poya Terrane [*Cluzel et al.*, 2001], are dissimilar to the amphibolites with LREE-depletion rather than enrichment and plotting on the high Nb/Y side of the subalkaline basalt field (Figure 8). Depleted MORBs (BABB-like) similar in chemistry to the amphibolites, are rare in the Poya Terrane; however, they represent the youngest (Paleocene or Early Eocene) components that were scraped off the South Loyalty Basin crust during subduction/obduction. These basalts share most of the geochemical features of type 1 amphibolites; e.g., LREE depletion (Figure 9), similar Nb/Y (Figure 8) and Nb/Ta ratios, a weak negative Nb anomaly, no noticeable Ta anomaly, and very low Th contents (Figure 10). Therefore, these rare BABB-like basalts of the Poya Terrane are a reasonable protolith for the type 1 amphibolites.

[62] The peak temperature conditions (850–980°C; Table S2) estimated from Eocene amphibolites are within the range of that advocated for the metamorphic sole of many ophiolites; in contrast, the estimated pressure (~0.5 GPa) is lower than of granulites that are a common component of metamorphic soles [*Searle and Cox*, 1999, 2002], and suggest that these rocks have never been dragged at great depth; or alternatively, have not been exhumed from the base of the upper plate, as most probably granulites do. The relatively high thermal gradient (~60°C.km^{-1}) recorded by amphibolites at ~56 Ma suggests that hot, i.e., young lithosphere was involved at beginning, and sharply contrasts with that

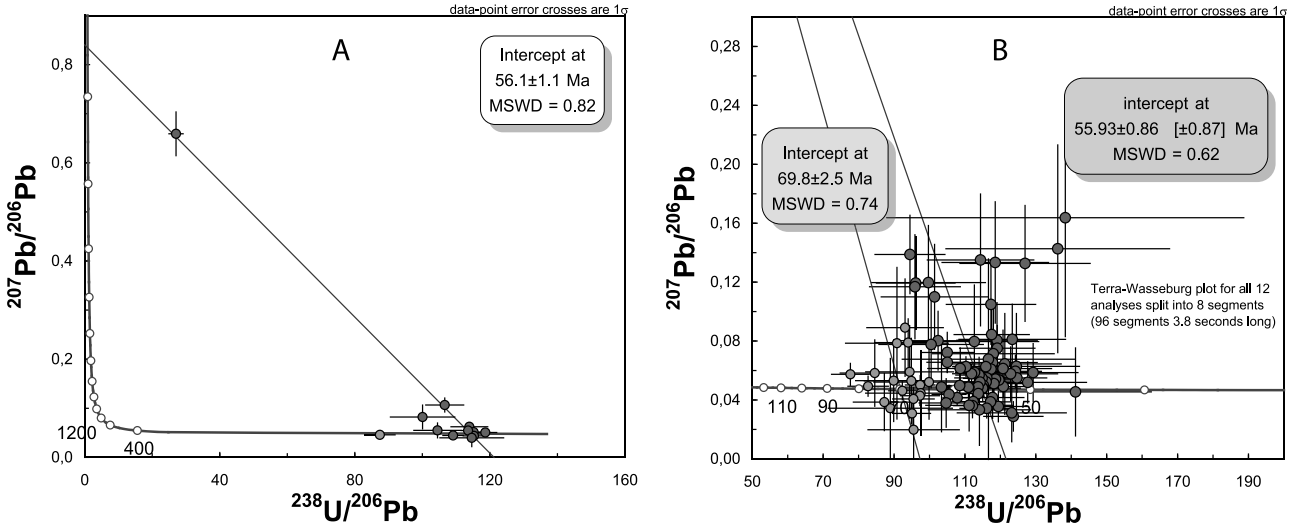

Figure 13. (a) Reverse concordia diagram (Tera–Wasserburg) showing the U/Pb isotopic ratios of 13 zircons analyzed from sample Mueo4 (felsic dyke). The majority of the data is near-concordant clustering at ~56 Ma (calculated by the isoplot program of *Ludwig* [2003]). (b) To check for possible discrepancies, each analysis has been split into segments 3.8 s long and provides two distinct intercepts at 69.8 ± 2.5 and 55.9 ± 0.8 Ma, respectively. Solid lines are mixing isochrons through the data anchored common Pb at 70 and 56 Ma, respectively [*Stacey and Kramers*, 1975].

recorded by eclogites and blueschists of Pouebo and Diahot terranes (~10°C.km^{-1}) [*Clarke et al.*, 1997; *Carson et al.*, 1999; *Fitzherbert et al.*, 2005]. Such low values infer that at ~44 Ma [*Spandler et al.*, 2005] a relatively cold thermal gradient prevailed in the subduction zone.

[63] The metamorphic and magmatic rocks associated with the Peridotite Nappe seem to track the cooling of the subduction zone over a 12 Ma period. At start, high-temperature metamorphism recorded by amphibolites at ~56 Ma probably closely followed subduction initiation. During the 53.2–49.6 Ma interval, slab melts (adakite-like) formed beneath the fore-arc as documented by *Cluzel et al.* [2006]. Finally, much cooler, high P/T conditions prevailed by 44 Ma as recorded by the eclogites. These data shed some light on the cooling of the subduction zone and suggest that subduction started at, or near an active ridge just prior to 56 Ma and involved an increasingly colder, i.e., older, lithosphere as the system progressed toward collision.

[64] The $^{40}Ar/^{39}Ar$ apparent age of hornblende in Pinjen amphibolite is indistinguishable within error from the zircon U-Pb age of Mueo amphibolite (Nepoui); therefore, if the two localities actually belong to the same unit (a very likely feature), cooling of amphibolite from ~900°C to ~550°C was extremely rapid and probably less than a few million years, a feature consistent with a metamorphic sole environment [*Hacker et al.*, 1996; *Wakabayashi and Dilek*, 2000].

[65] The Early Eocene events documented here are very close (<2 Ma) but yet different to Late Paleocene (57.8 to 58.6 Ma) $^{40}Ar/^{39}Ar$ ages from amphibolites in the sole of the Papuan Ultramafic Complex now 2000 km to the northeast [*Lus et al.*, 2004] suggesting some sort of regional geodynamic link. However, links to broader geodynamic plate or hot spot movement changes such as those responsible for the bend in the Emperor-Hawaii island and seamount chain [see *Whattam et al.*, 2008; *Whattam*, 2009] are unlikely because $^{40}Ar/^{39}Ar$ and U-Pb ages presented in this study are significantly older, and the real cause of subduction inception remains unknown.

9. Conclusion

[66] The new geochronological and geochemical data on the amphibolites at the base of the Ophiolite Nappe in New Caledonia combined with data from earlier studies supports a model for the initiation of subduction prior to ~56 Ma at the same time as the youngest Poya Terrane basalt were erupted. It is worth noting that the BABB protolith (and the rest of Poya Terrane as well) has been generated in a different setting and represents the latest stage of Late Cretaceous-Eocene marginal basin opening (Figure 14a) (for details see *Cluzel et al.* [2001, 2010]). It is however worth noting that no trace of a Late Cretaceous-Eocene arc has been hitherto discovered, and that occurrence of a west-dipping subduction remains conjectural. These BABB-type rocks recrystallized into high-temperature amphibolite facies as they were reworked into a newly formed subduction zone with an opposite polarity. This was followed from 54.8 to 49.6 Ma by intrusion of slab-derived melts within the fore-arc mantle section, now represented by the Peridotite Nappe. Such a coincidence suggests that northward or northeastward subduction of the South Loyalty Basin started at, or close to, the spreading ridge at ≥56 Ma (Figure 14a). Slab melts, and IAT dolerites intruded the fore-arc mantle section at ~53 Ma (Figures 14b and 14c). Very shortly afterwards (at ~49 Ma), the fore-arc was "frozen" (Figure 14d), and a new HP-LT thermal regime progressively established in the subduction zone, while the magmatic activity most probably migrated into the Loyalty Arc. The final stage of the evolution of this subduction zone occurred when the Norfolk (New Caledonia) Ridge blocked the subduction, and caused

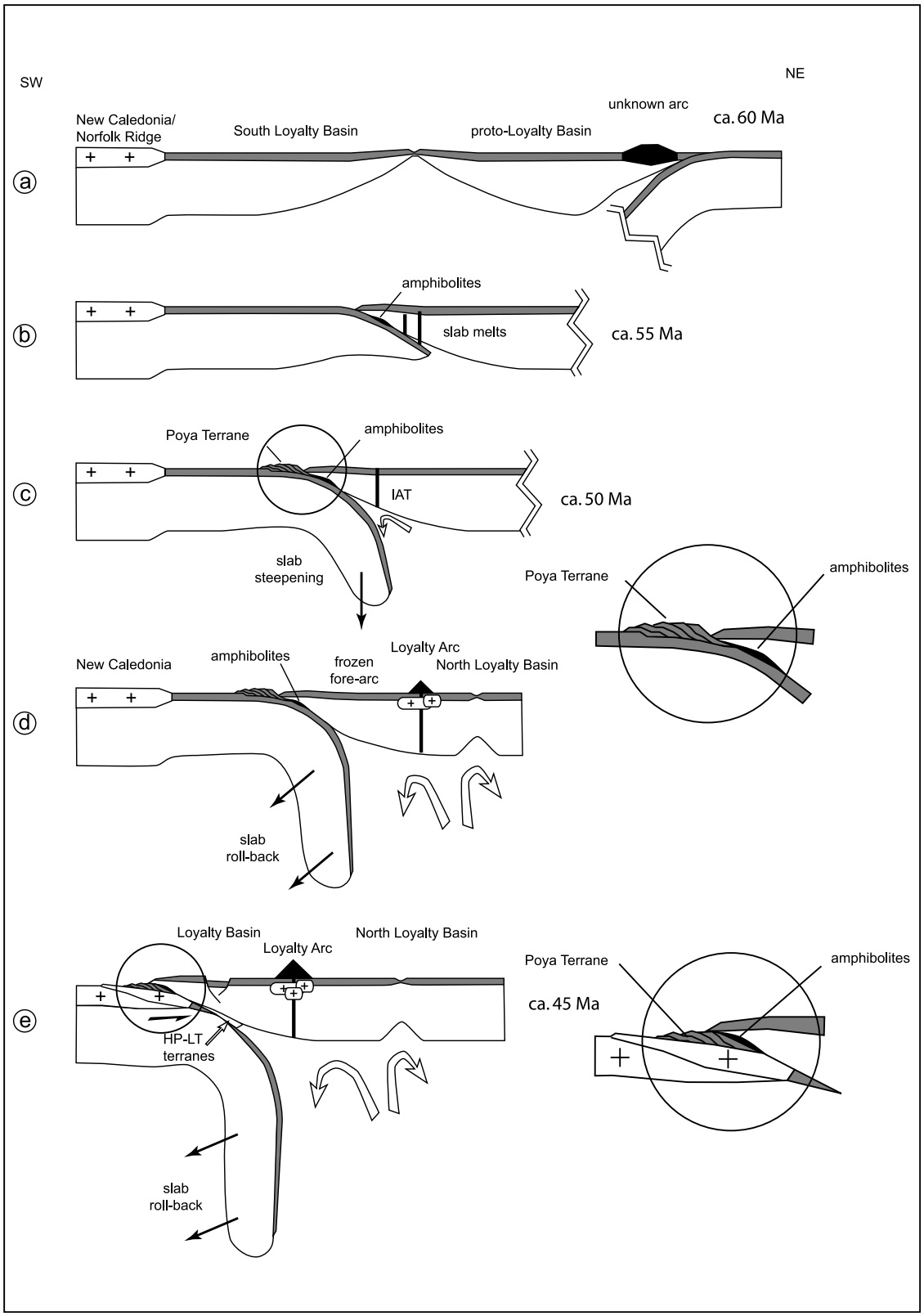

Figure 14. (a–e) A tentative summary of the evolution of New Caledonia from subduction inception (earliest Eocene) to obduction (latest Eocene). It is worth noting that subduction and obduction were oblique with respect to the limits of Norfolk/New Caledonia Ridge [see *Cluzel et al.*, 2001], and that a cross section is unable to represent the process satisfactorily. This model is mainly based upon *Cluzel et al.* [1999, 2001] and only completed for amphibolites.

the obduction of the oceanic lithosphere of the Loyalty Basin onto the ridge (Figure 14e) (details of Figures 14d and 14e come from the model developed in *Cluzel et al.* [1999, 2001, 2006] and *Paquette and Cluzel* [2007]).

[67] The polarity of the HP-LT metamorphic units, southward in-sequence thrusting and migrating foreland basins, occurrence of high-temperature amphibolite lenses and fore-arc slab melt rocks, all suggest that Late Eocene obduction in New Caledonia was preceded by a northeast or north-northeast-dipping subduction. This new subduction was probably born just before 56 Ma, owing to the latency period (~0.25 Ma) necessary for reaching the peak metamorphic conditions at ~56 Ma, and generating the early melts at ~53 Ma. It continued at least in New Caledonia, during the 56–34 Ma period.

[68] **Acknowledgments.** A. Frew is thanked for help with the $^{40}Ar/^{39}Ar$ analyses, and T. Holmes is thanked for heavy mineral separation. Special thanks are due to J. Wakabayashi for an extensive and constructive review of an early version of this article and to the Associate Editor M. Rusmore for her very useful comments. J. Wakabayashi and L. Jolivet are also thanked for reviewing the second version.

References

Aitchison, J. C., G. L. Clarke, D. Cluzel, and S. Meffre (1995a), Eocene arc-continent collision in New Caledonia and implications for regional southwest Pacific tectonic evolution, *Geology*, *23*, 161–164, doi:10.1130/0091-7613(1995)023<0161:EACCIN>2.3.CO;2.

Aitchison, J. C., S. Meffre, and D. Cluzel (1995b), Cretaceous/Tertiary Radiolarians from New Caledonia, *Geol. Soc. N. Z. Misc. Publ. 81A*, 70 pp., Geol. Soc. of N. Z., Wellington, New Zealand.

Aitchison, J. C., T. R. Ireland, G. L. Clarke, D. Cluzel, and S. Meffre (1998), U/Pb SHRIMP age constraints on the tectonic evolution of New Caledonia and regional implications, *Tectonophysics*, *299*, 333–343, doi:10.1016/S0040-1951(98)00211-X.

Anderson, J. L., and D. R. Smith (1995), The effects of temperature and fO_2 on the Al-in-hornblende barometer, *Am. Mineral.*, *80*, 549–559.

Audet, M. A. (2008), Le massif du Koniambo, Nouvelle-Calédonie: Formation et obduction d'un complexe ophiolitique du type SSZ. Enrichissement en nickel, cobalt et scandium dans les profils résiduels, PhD thesis, 327 pp., Univ. of New Caledonia, Nouméa, New Caledonia.

Avias, J. (1967), Overthrust structure of the main ultrabasic New Caledonian massives, *Tectonophysics*, *4*, 531–541, doi:10.1016/0040-1951(67)90017-0.

Baldwin, S. L., T. Rawlings, and P. G. Fitzgerald (2007), Thermochronology of the New Caledonian high-pressure terrane: Implications for middle Tertiary plate boundary processes in the Southwest Pacific, in *Convergent Margin Terranes and Associated Regions: A Tribute to W. G. Erns*, edited by M. Cloos et al., *Spec. Pap. Geol. Soc. Am.*, *419*, 117–134, doi:10.1130/2006.2419(06).

Berggren, W. A., and P. N. Pearson (2005), A revised tropical to subtropical Paleogene planktonic foraminiferal zonation, *J. Foraminiferal Res.*, *35*(4), 279–298, doi:10.2113/35.4.279.

Berggren, W. A., D. V. Kent, C. C. Swisher III, and M.-P. Aubry (1995), A revised Cenozoic geochronology and chronostratigraphy, in *Geochronology, Time Scales and Stratigraphic Correlation*, edited by W. A. Berggren et al., *Spec. Publ. SEPM Soc. Sediment. Geol.*, *54*, 129–212.

Bodinier, J. L., C. Merlet, R. M. Bedini, F. Simien, M. Remaidi, and C. J. Garrido (1996), Distribution of niobium, tantalium, and other highly incompatible trace elements in the lithospheric mantle: The spinel paradox, *Geochim. Cosmochim. Acta*, *60*, 545–550, doi:10.1016/0016-7037(95)00431-9.

Boudier, F., and A. Nicolas (2007), Comment on "dating the geologic history of Oman's Semail ophiolite: Insights from U–Pb geochronology" by C. J. Warren, R. R. Parrish, D. J. Waters and M. P. Searle, *Contrib. Mineral. Petrol.*, *154*, 111–113, doi:10.1007/s00410-007-0189-5.

Boudier, F., G. Ceuleneer, and A. Nicolas (1988), Shear zones, thrusts and related magmatism in the Oman ophiolite: Initiation of thrusting on an oceanic ridge, *Tectonophysics*, *151*, 275–296, doi:10.1016/0040-1951(88)90249-1.

Carroué, J. P. (1972), Carte géologique de la Nouvelle-Calédonie au 1/50 000è, feuille Pouembout, map, Bur. de Rech. Geol. et Min., Paris.

Carson, C. J., R. Powell, and G. L. Clarke (1999), Calculated mineral equilibria for eclogites in CaO-Na2O-FeO-MgO-Al2O3-SiO2–H2O; application to the Pouebo Terrane, Pam peninsula, New Caledonia, *J. Metamorph. Geol.*, *17*, 9–24, doi:10.1046/j.1525-1314.1999.00177.x.

Carson, C. J., G. L. Clarke, and R. Powell (2000), Hydration of eclogite, Pam Peninsula, New Caledonia, *J. Metamorph. Geol.*, *18*, 79–90, doi:10.1046/j.1525-1314.2000.00245.x.

Chemenda, A. I., M. Mattauer, and A. N. Bokun (1996), Continental subduction and a mechanism for exhumation of high-pressure metamorphic rocks: New modelling and field data from Oman, *Earth Planet. Sci. Lett.*, *143*(1–4), 173–182, doi:10.1016/0012-821X(96)00123-9.

Clarke, G., J. C. Aitchison, and D. Cluzel (1997), Eclogites and blueschists of the Pam Peninsula, NE New Caledonia: A reappraisal, *J. Petrol.*, *38*(7), 843–876.

Cluzel, D., and S. Meffre (2002), L'unité de la Boghen (Nouvelle-Calédonie, Pacifique sud-ouest): Un complexe d'accrétion jurassique. Données radiochronologiques préliminaires U-Pb sur les zircons détritiques. *C. R. Geosci.*, *334*, 867–874.

Cluzel, D., J. Aitchison, G. Clarke, S. Meffre, and C. Picard (1994), Point de vue sur l'évolution tectonique et géodynamique de la Nouvelle-Calédonie, *C. R. Acad. Sci., Ser. IIA*, *319*, 683–688.

Cluzel, D., C. Picard, J. C. Aitchison, C. Laporte, S. Meffre, and F. Parat (1997), La Nappe de Poya (ex-Formation des basaltes) de Nouvelle-Calédonie (Pacifique sud-ouest), un plateau océanique Campanien-Paléocène supérieur obducté à l'Eocène supérieur, *C. R. Acad. Sci., Ser. IIA*, *324*, 443–451.

Cluzel, D., D. Chiron, and M. D. Courme (1998), Discordance de l'Eocène supérieur et événements pré-obduction en Nouvelle-Calédonie (Pacifique sud-ouest), *C. R. Acad. Sci., Ser. IIA*, *327*, 485–491, doi:10.1016/S1251-8050(99)80077-9.

Cluzel, D., J. C. Aitchison, P. M. Black, and C. Picard (1999), Origin and fate of Southwest Pacific marginal basins: An appraisal from New Caledonia, paper presented at Mid-Cretaceous to Recent Plate Boundary Processes in the Southwest Pacific,'99 Penrose Conference, Geol. Soc. of Am., Arthur's Pass, New Zealand.

Cluzel, D., J. C. Aitchison, and C. Picard (2001), Tectonic accretion and underplating of mafic terranes in the Late Eocene intraoceanic fore-arc of New Caledonia (Southwest Pacific). Geodynamic implications, *Tectonophysics*, *340*(1–2), 23–59, doi:10.1016/S0040-1951(01)00148-2.

Cluzel, D., S. Meffre, P. Maurizot, and A. J. Crawford (2006), Earliest Eocene (53 Ma) convergence in the Southwest Pacific; evidence from pre-obduction dikes in the ophiolite of New Caledonia, *Terra Nova*, *18*, 395–402, doi:10.1111/j.1365-3121.2006.00704.x.

Cluzel, D., C. J. A. Adams, S. Meffre, H. Campbell, and P. Maurizot (2010), Discovery of Early Cretaceous rocks in New Caledonia (Southwest Pacific). New geochemical and U-Pb zircon age constraints on the transition from subduction to marginal breakup, *J. Geol.*, *118*(4), 381–397, doi:10.1086/652779.

Coleman, R. G. (1971), Plate tectonic emplacement of upper mantle peridotites along continental edges, *J. Geophys. Res.*, *76*(5), 1212–1222, doi:10.1029/JB076i005p01212.

Collot, J. Y., A. Malahoff, J. Recy, G. Latham, and F. Missegue (1987), Overthrust emplacement of New Caledonia ophiolite: Geophysical evidence, *Tectonics*, *6*, 215–232, doi:10.1029/TC006i003p00215.

Crawford, A. J., S. Meffre, and P. A. Symonds (2003), 120 to 0 Ma tectonic evolution of the Southwest Pacific and analogous geological evolution of the 600 to 220 Ma Tasman Fold Belt System, in *Evolution and Dynamics of the Australian Plate*, edited by R. R. Hillis and R. D. Müller, *Spec. Pap. Geol. Soc. Am.*, *22*, 377–397.

Dilek, Y. (2003), Ophiolite concept and its evolution, in *Ophiolite Concept and the Evolution of Geological Thought*, edited by Y. Dilek and S. Newcomb, *Spec. Pap. Geol. Soc. Am.*, *373*, 1–16.

Eissen, J. P., A. J. Crawford, J. Cotten, S. Meffre, H. Bellon, and M. Delaune (1998), Geochemistry and tectonic significance of basalts in the Poya Terrane, New Caledonia, *Tectonophysics*, *284*, 203–219, doi:10.1016/S0040-1951(97)00183-2.

Ernst, J. G., and J. Liu (1998), Experimental phase-equilibrium study of Al- and Ti-contents of calcic amphibole in MORB—A semiquantitative thermobarometer, *Am. Mineral.*, *83*, 952–969.

Evensen, N. M., P. J. Hamilton, and R. K. O'Nions (1978), Rare earth abundance in chondritic meteorites, *Geochim. Cosmochim. Acta*, *42*, 1199–1212, doi:10.1016/0016-7037(78)90114-X.

Fitzherbert, J. A., G. L. Clarke, and R. Powell (2003), Lawsonite–omphacite–bearing metabasites of the Pam Peninsula, NE New Caledonia: Evidence for disrupted blueschist– to eclogite–facies conditions, *J. Petrol.*, *44*, 1805–1831, doi:10.1093/petrology/egg060.

Fitzherbert, J. A., G. L. Clarke, and R. Powell (2005), Preferential retrogression of high-P metasediments and the preservation of blueschist to eclogite facies metabasite during exhumation, Diahot terrane, NE New Caledonia, *Lithos*, *83*, 67–96, doi:10.1016/j.lithos.2005.01.005.

Frost, B. R., K. R. Chamberlain, and J. C. Schumacher (2001), Sphene (titanite): Phase relations and role as a geochronometer, *Chem. Geol.*, *172*(1–2), 131–148, doi:10.1016/S0009-2541(00)00240-0.

Ghatak, A., A. R. Basu, and J. Wakabayashi (2012), Elemental Mobility in Subduction Metamorphism: Insight from metamorphic rocks of the Franciscan Complex and the Feather River ultramafic belt, California, *Int. Geol. Rev.*, *54*(6), 654–685, doi:10.1080/00206814.2011.567087.

Hacker, B. R., J. L. Mosenfelder, and E. Gnos (1996), Rapid emplacement of the Oman ophiolite: Thermal and geochronologic constraints, *Tectonics*, *15*, 1230–1247, doi:10.1029/96TC01973.

Holland, T., and J. Blundy (1994), Non-ideal interactions in calcic amphiboles and their bearing on amphibole-plagioclase thermometry, *Contrib. Mineral. Petrol.*, *116*, 433–447, doi:10.1007/BF00310910.

Jourdan, F., and P. R. Renne (2007), Age calibration of the Fish Canyon sanidine $^{40}Ar/^{39}Ar$ dating standard using primary K-Ar standards, *Geochim. Cosmochim. Acta*, *71*, 387–402, doi:10.1016/j.gca.2006.09.002.

Kalfoun, F., D. Ionov, and C. Merlet (2002), HFSE residence and Nb/Ta ratios in metasomatised, rutile-bearing mantle peridotites, *Earth Planet. Sci. Lett.*, *199*, 49–65, doi:10.1016/S0012-821X(02)00555-1.

Langmuir, C. H., A. Bézos, S. Escrig, and S. W. Parman (2006), Chemical systematics and hydrous melting of the mantle in back-arc basins, in *Back-Arc Spreading Systems: Geological, Biological, Chemical, and Physical Interactions*, *Geophys. Monogr. Ser*, vol. 166, edited by D. M. Christie et al., pp. 87–146, AGU, Washington, D. C., doi:10.1029/166GM07

Le Bas, M. J., R. W. Le Maitre, A. Streckeisen, and B. Zanettin (1986), A chemical classification of volcanic rocks based on the total alkali–silica diagram, *J. Petrol.*, *27*, 745–750.

Leake, B. E., et al. (1997), Nomenclature of amphiboles, *Am. Mineral.*, *82*, 1019–1037.

Lehnert, K., Y. Su, C. Langmuir, B. Sarbas, and U. Nohl (2000), A global geochemical database structure for rocks, *Geochem. Geophys. Geosyst.*, *1*(5), 1012, doi:10.1029/1999GC000026.

Lippard, S. J. (1983), Cretaceous high pressure metamorphism in NE Oman and its relationship to subduction and ophiolite nappe emplacement, *J. Geol. Soc.*, *140*, 97–104, doi:10.1144/gsjgs.140.1.0097.

Ludwig, K. R. (2003), User's manual for Isoplot 3.00: A geochronological toolkit for Microsoft Excel, *Berkeley Geochronol. Cent. Spec. Publ. 4*, Berkeley Geochronol. Cent., Berkeley, Calif.

Lus, W. Y., I. McDougall, and H. L. Davies (2004), Age of the metamorphic sole of the Papuan Ultramafic Belt ophiolite, Papua New Guinea, *Tectonophysics*, *392*(1–4), 85–101, doi:10.1016/j.tecto.2004.04.009.

Marchesi, C., C. J. Garrido, M. Godard, F. Belley, and E. Ferré (2009), Migration and accumulation of ultra-depleted subduction-related melts in the Massif du Sud ophiolite (New Caledonia), *Chem. Geol.*, *266*, 171–186, doi:10.1016/j.chemgeo.2009.06.004.

Maurizot, P. (2011), Premiers enregistrements sédimentaires de la convergence pré-obduction en Nouvelle-Calédonie: Formation d'un complexe d'accrétion à l'Eocène inférieur dans le Nord de la Grande-Terre et mise en place de la nappe des Montagnes Blanches, *Bull. Soc. Geol. Fr.*, *182*, 479–491, doi:10.2113/gssgfbull.182.6.479.

Meffre, S., J. C. Aitchison, and A. J. Crawford (1996), Geochemical stratigraphy of boninites and tholeiites from the Permo-Triassic Koh Ophiolite, New Caledonia, *Tectonics*, *15*, 67–83, doi:10.1029/95TC02316.

Nicholson, K. N., C. Picard, and P. M. Black (2000), A comparative study of Late Cretaceous ophiolitic basalts from New Zealand and New Caledonia: Implications for the tectonic evolution of the SW Pacific, *Tectonophysics*, *327*, 157–171, doi:10.1016/S0040-1951(00)00167-0.

Nicolas, A. (1989), *Structures of Ophiolites and Dynamics of Oceanic Lithosphere*, 367 pp., Kluwer Acad., Amsterdam.

Otten, M. T. (1984), The origin of brown hornblende in the Artfjället gabbro and dolerites, *Contrib. Mineral. Petrol.*, *86*(2), 189–199, doi:10.1007/BF00381846.

Paquette, J. L., and D. Cluzel (2007), U–Pb zircon dating of post-obduction volcanic-arc granitoids and a granulite-facies xenolith from New Caledonia. Inference on Southwest Pacific geodynamic models, *Int. J. Earth Sci.*, *96*, 613–622, doi:10.1007/s00531-006-0127-1.

Paris, J. P. (1981), *Géologie de la Nouvelle-Calédonie. Un essai de synthèse*, *Mem. BRGM*, *113*, 278 pp.

Parrot, J. F., and F. Dugas (1980), The disrupted ophiolitic belt of the Southwest Pacific: Evidence for an Eocene subduction zone, *Tectonophysics*, *66*, 349–372, doi:10.1016/0040-1951(80)90249-8.

Peacock, S. M., T. Rushmer, and A. B. Thompson (1994), Partial melting of subducting oceanic crust, *Earth Planet. Sci. Lett.*, *121*, 227–244, doi:10.1016/0012-821X(94)90042-6.

Pearce, J. A. (1982), Trace element characteristics of lavas from destructive plate margins, in *Orogenic Andesites and Related Rocks*, edited by R. S. Thorpe, pp. 525–548, John Wiley, Chichester, U. K.

Pearce, J. A. (1996), A user's guide to basalt discrimination diagrams, in *Trace Element Geochemistry of Volcanic Rocks: Applications for Massive Sulphide Exploration*, *Short Course Notes*, vol. 12, edited by D. A. Wyman, pp. 79–113, Geol. Assoc. of Can., St. John's, Newfoundland Labrador, Canada.

Platt, J. P. (1993), Exhumation of high-pressure rocks: A review of concepts and processes, *Terra Nova*, *5*(2), 119–133, doi:10.1111/j.1365-3121.1993.tb00237.x.

Poli, S. (1993), The amphibolite-eclogite transformation: An experimental study on basalt, *Am. J. Sci.*, *293*, 1061–1107, doi:10.2475/ajs.293.10.1061.

Prinzhoffer, A. (1981), Structure et pétrologie d'un cortège ophiolitique: Le massif du Sud (Nouvelle-Calédonie), PhD thesis, Ec. Natl. Super. des Mines des Paris, Paris.

Prinzhoffer, A. (1987), Processus de fusion dans les zones d'extension océaniques et continentals, PhD thesis, 237 pp., Univ. Paris VII, Paris.

Renne, P. R., R. Mundil, G. Balco, K. Min, and K. R. Ludwig (2010), Joint determination of ^{40}K decay constants and $^{40}Ar^*/^{40}K$ for the Fish Canyon sanidine standard, and improved accuracy for $^{40}Ar/^{39}Ar$ geochronology, *Geochim. Cosmochim. Acta*, *74*, 5349–5367, doi:10.1016/j.gca.2010.06.017.

Robertson, A. (2004), Development of concepts concerning the genesis and emplacement of Tethyan ophiolites in the Eastern Mediterranean and Oman regions, *Earth Sci. Rev.*, *66*, 331–387, doi:10.1016/j.earscirev.2004.01.005.

Schellart, W. P., G. S. Lister, and V. G. Toy (2006), A Late Cretaceous and Cenozoic reconstruction of the Southwest Pacific region: Tectonics controlled by subduction and slab rollback processes, *Earth Sci. Rev.*, *76*(3–4), 191–233, doi:10.1016/j.earscirev.2006.01.002.

Schmidt, M. W. (1992), Amphibole composition in tonalite as a function of pressure: an experimental calibration of the Al-in-hornblende barometer, *Contrib. Mineral. Petrol.*, *110*(2–3), 304–310, doi:10.1007/BF00310745.

Searle, M. P., and J. Cox (1999), Tectonic setting, origin, and obduction of the Oman ophiolite, *Geol. Soc. Am. Bull.*, *111*, 104–122, doi:10.1130/0016-7606(1999)111<0104:TSOAOO>2.3.CO;2.

Searle, M. P., and J. Cox (2002), Subduction zone metamorphism during formation and emplacement of the Semail ophiolite in the Oman Mountains, *Geol. Mag.*, *139*(3), 241–255, doi:10.1017/S0016756802006532.

Smart, C. M., and J. Wakabayashi (2009), Hot and deep: Rock record of subduction initiation and exhumation of high-temperature, high-pressure metamorphic rocks, Feather River ultramafic belt, California, *Lithos*, *113*, 292–305, doi:10.1016/j.lithos.2009.06.012.

Spandler, C., J. Hermann, R. Arculus, and J. Mavrogenes (2004), Geochemical heterogeneity and element mobility in deeply subducted oceanic crust; insights from high-pressure mafic rocks from New Caledonia, *Chem. Geol.*, *206*, 21–42, doi:10.1016/j.chemgeo.2004.01.006.

Spandler, C., D. Rubatto, and J. Hermann (2005), Late Cretaceous-Tertiary tectonics of the southwest Pacific: Insights from U-Pb sensitive, high-resolution ion microprobe (SHRIMP) dating of eclogite facies rocks from New Caledonia, *Tectonics*, *24*, TC3003, doi:10.1029/2004TC001709.

Stacey, J. S., and J. D. Kramers (1975), Approximation of terrestrial lead isotope evolution by a two-stage model, *Earth Planet. Sci. Lett.*, *26*(2), 207–221, doi:10.1016/0012-821X(75)90088-6.

Sun, S. S., and W. I. McDonough (1989), Chemical and isotopic systematics of oceanic basalts: Implications for mantle composition and processes, in *Magmatism in the Ocean Basins*, edited by A. D. Saunders and M. D. Norry, *Geol. Soc. Spec. Publ.*, *42*, pp. 313–345, doi:10.1144/GSL.SP.1989.042.01.19.

Sutherland, R., et al. (2010), Lithosphere delamination with foundering of lower crust and mantle caused permanent subsidence of New Caledonia Trough and transient uplift of Lord Howe Rise during Eocene and Oligocene initiation of Tonga-Kermadec subduction, western Pacific, *Tectonics*, *29*, TC2004, doi:10.1029/2009TC002476.

Tiepolo, M., R. Vannucci, R. Oberti, S. Foley, P. Bottazzi, and A. Zanetti (2000), Nb and Ta incorporation and fractionation in titanian pargasite and kaersutite: Crystal-chemical constraints and implications for natural systems, *Earth Planet. Sci. Lett.*, *176*, 185–201, doi:10.1016/S0012-821X(00)00004-2.

Ulrich, M., C. Picard, S. Guillot, C. Chauvel, D. Cluzel, and S. Meffre (2010), Multiple melting stages and refertilisation process as indicators for ridge to subduction formation: The New Caledonia Ophiolite, *Lithos*, *115*, 223–236, doi:10.1016/j.lithos.2009.12.011.

Villa, I. M., B. Grobéty, S. P. Kelley, R. Trigila, and R. Wieler (1996), Assessing Ar transport paths and mechanisms for McClure Mountains Hornblende, *Contrib. Mineral. Petrol.*, *126*, 67–80, doi:10.1007/s004100050236.

Wakabayashi, J., and Y. Dilek (2000), Spatial and temporal relationships between ophiolites and their metamorphic soles: A test of fore-arc ophiolite genesis, in *Ophiolites and Oceanic Crust: New Insights From Field*

Studies and the Ocean Drilling Program, edited by Y. Dilek et al., *Spec. Pap. Geol. Soc. Am.*, *349*, 53–64.

Wakabayashi, J., and Y. Dilek (2003), What constitutes 'emplacement' of an ophiolite?: Mechanisms and relationship to subduction initiation and formation of metamorphic soles, in *Ophiolites in Earth History*, edited by Y. Dilek and R. T. Robinson, *Geol. Soc. Lond. Spec. Publ.*, *218*, 427–447, doi:10.1144/GSL.SP.2003.218.01.22.

Wakabayashi, J., A. Ghatak, and A. R. Basu (2010), Suprasubduction-zone ophiolite generation, emplacement, and initiation of subduction: A perspective from geochemistry, metamorphism, geochronology, and regional geology, *Geol. Soc. Am. Bull.*, *122*, 1548–1568, doi:10.1130/B30017.1.

Whattam, S. A. (2009), Arc-continent collisional orogenesis in the SW Pacific and the nature, source and correlation of emplaced ophiolitic nappe components, *Lithos*, *113*, 88–114, doi:10.1016/j.lithos.2008.11.009.

Whattam, S. A., J. Malpas, J. R. Ali, and I. E. M. Smith (2008), New SW Pacific tectonic model: Cyclical intraoceanic magmatic arc construction and near-coeval emplacement along the Australia-Pacific margin in the Cenozoic, *Geochem. Geophys. Geosyst.*, *9*, Q03021, doi:10.1029/2007GC001710.

Winchester, J. A., and P. A. Floyd (1977), Geochemical discrimination of different magma series and their differentiation products using immobile elements, *Chem. Geol.*, *20*, 325–343, doi:10.1016/0009-2541(77)90057-2.

Yamato, P., P. Agard, B. Goffé, V. De Andrade, O. Vidal, and L. Jolivet (2007), New, high-precision P-T estimates for Oman blueschists: Implications for obduction, nappe stacking and exhumation processes, *J. Metamorph. Geol.*, *25*, 657–682, doi:10.1111/j.1525-1314.2007.00722.x.